SMALL, LOW-COST, EXPENDABLE TURBOJET ENGINE

I - Design, Fabrication, and Preliminary Testing

Robert P. Dengler and Lawrence E. Macioce

Lewis Research Center
Cleveland, Ohio 44135

1. Report No. NASA TM X-3392	2. Government Accession No.	3. Recipient's Catalog No.
4. Title and Subtitle SMALL, LOW-COST, EXPENDABLE TURBOJET ENGINE I - DESIGN, FABRICATION, AND PRELIMINARY TESTING		5. Report Date May 1976
		6. Performing Organization Code
7. Author(s) Robert P. Dengler and Lawrence E. Macioce		8. Performing Organization Report No. E-8590
9. Performing Organization Name and Address Lewis Research Center National Aeronautics and Space Administration Cleveland, Ohio 44135		10. Work Unit No. 505-04
		11. Contract or Grant No.
12. Sponsoring Agency Name and Address National Aeronautics and Space Administration Washington, D. C. 20546		13. Type of Report and Period Covered Technical Memorandum
		14. Sponsoring Agency Code

15. Supplementary Notes

16. Abstract

A small experimental axial-flow turbojet engine in the 2669-newton (600-lbf) thrust class was designed, fabricated, and tested to demonstrate the feasibility of several low-cost concepts. Design simplicity was stressed in order to reduce the number of components and machining operations. Four engines were built and tested for a total of 157 hours. Engine testing was conducted at both sea-level static and simulated flight conditions for engine speeds as high as 38 000 rpm and turbine-inlet temperatures as high as 1255 K (1800° F).

17. Key Words (Suggested by Author(s)) Turbojet engines Turbine engines Gas turbine engines	18. Distribution Statement Unclassified - unlimited STAR Category 07 (rev.)		
19. Security Classif. (of this report) Unclassified	20. Security Classif. (of this page) Unclassified	21. No. of Pages 51	22. Price* $4.50

SMALL, LOW-COST, EXPENDABLE TURBOJET ENGINE

I - DESIGN, FABRICATION, AND PRELIMINARY TESTING

by Robert P. Dengler and Lawrence E. Macioce

Lewis Research Center

SUMMARY

A small experimental turbojet engine was designed and fabricated to demonstrate the feasibility of some low-cost concepts that were studied at NASA-Lewis. The engine design was intended for an expendable application but some of its features may also be considered for light, subsonic aircraft applications. The basic design was that of an axial-flow turbojet engine with a four-stage compressor, an annular combustor, a single-stage turbine, and a fixed-area exhaust nozzle. The engine had a maximum diameter of 29 centimeters ($11\frac{1}{2}$ in.) and an overall length of 96.5 centimeters (38 in.); it weighed about 59 kilograms (130 lbm). It was designed with a compressor pressure ratio of 4.0 and was expected to produce a thrust of 2669 newtons (600 lbf) at sea-level static conditions.

Design simplicity was stressed to reduce whenever possible the number of components, handling, and machining operations required. The design incorporated the extensive use of casting for most of the main engine components, and featured an all-welded compressor rotor mainshaft assembly, a simplified combustor assembly, an oil-mist bearing-lubrication system, a simplified fuel-pump – fuel-control assembly, and a compressor-turbine rotor simply supported through a soft-mounted, two-main-bearing system.

Preliminary full-scale engine tests revealed the need for modifications to the compressor blading geometry, the turbine stator throat area, and the bearing mount, which were subsequently corrected. The engine starting characteristics are presented along with the engine operating lines for testing conducted with three different exhaust nozzle sizes. Four engines were built and tested for a total of 157 hours. Engine testing was conducted at both sea-level-static and simulated flight conditions at engine speeds as high as 38 000 rpm and turbine-inlet temperatures as high as 1255 K (1800° F). Simulated flight tests included operation at Mach numbers as high as 1.2 and altitudes as high as 9144 meters (30 000 ft). On successful completion of all test requirements, two engine assemblies were delivered to the Naval Weapons Center for their own demonstration testing.

INTRODUCTION

This report presents a description and some general operating characteristics of a small, low-pressure-ratio experimental turbojet engine, designed and fabricated for an expendable application. The intent was for this engine to be a demonstrator of low-cost concepts under study at Lewis. Although these concepts were intended for expendable aircraft, such as drones or remote piloted vehicles (RPV's), in some cases they would apply to light subsonic aircraft as well.

Gas turbine engines are now commonplace in both military and commercial aircraft. Two fields where gas-turbine engines are rare, however, are general aviation and military missile applications where the engine powerplant is considered expendable. The small size and weight of gas turbine engines makes them attractive for use in these applications, but the very high cost of current gas turbine engines substantially restricts their use. The substitution of low-cost gas turbine engines for rocket engines presently being used on some missile applications appears particularly attractive because it would extend or improve the payload and range capability as well as result in a significant cost savings. The single mission and short-life requirements of engines for drones and missiles make possible major simplifications in the construction of such engines.

Several studies at Lewis have examined the feasibility of a low-cost, simplified version of a small gas turbine engine for use in light subsonic aircraft. References 1 to 3 present analytical, parametric studies of design and off-design performance characteristics for candidate turbofan and turbojet engine configurations. Based on performance and geometry, the turbojet engine was chosen for further study, and subsequently a contract was awarded to an engine manufacturer to provide engineering drawings of a turbojet engine. The engine design was to incorporate several cost reducing concepts that were being investigated at Lewis at that time. Some of these concepts are described in references 4 and 5. In addition, a new, simplified approach for a fuel control (refs. 6 to 8) was to be integrated into the basic engine design.

Shortly after a simplified, low-cost, man-rated engine design in the 4450-newton (1000-lbf) thrust class had been completed (ref. 9), the Naval Weapons Center at China Lake, California, expressed a need for an expendable turbojet engine of a somewhat smaller size, but including similar low-cost features. A joint program resulted in which Lewis agreed to provide the Naval Weapons Center (NWC) with an experimental turbojet engine for their use in flight tests to demonstrate the feasibility of replacing the rocket engine in a missile application. The expendable nature of this application permitted additional engine design simplifications which are described in reference 10.

Using this scaled-down design, the components of four engines were fabricated and assembled in accordance with the aforementioned economy approach. Initial testing was conducted for developmental purposes or the optimization of overall engine per-

formance characteristics. This preliminary testing was conducted at sea-level-static conditions primarily to determine proper compressor stator setting angles and exhaust nozzle areas.

BASIC LOW-COST ENGINE DESIGN APPROACH

The goal of gas-turbine engine designs of previous years has been to attain maximum performance in the form of either a high thrust-to-weight ratio or a low specific-fuel consumption. Such designs involve costly materials and expensive and time-consuming fabrication techniques, machining operations, and assembly procedures. To allow the widespread use of small gas turbine engines in applications such as general aviation or expendable powerplants in drones or missiles, costly materials and fabrication methods must be kept to a minimum. The basic design for a low-cost engine should incorporate economical approaches and be simple. By nature, this premise generally implies a trade-off of performance for lower costs; usually resulting in a somewhat higher specific-fuel consumption or lower thrust-to-weight ratio. For the applications being considered, however, this performance trade-off is generally acceptable.

The basic approach for the low-cost engine design was to (1) limit the design temperature to a level low enough to allow the use of low-cost materials, (2) limit the pressure ratio to reduce tip speed, stress levels, and the number of stages required, and (3) otherwise simplify the design to minimize the number of total engine parts and to reduce the amount of machining required without sacrificing reliability.

ENGINE DESIGN AND DESCRIPTION

General

The basic design criteria for this engine (including heat transfer and vibration analyses) is presented in references 9 and 10. By and large, the design is the direct scaling (by a factor of 0.72) of a somewhat larger engine design that had been completed and which was originally intended for lightweight, subsonic, man-rated aircraft. The short life and single mission requirements for the missile application did, however, permit some additional simplifications. In general, the basic requirements for the scaled-down design version were that it be

(1) Small - 30.5 centimeters (12 in.) in diameter and 96.5 centimeters (38 in.) long

(2) Relatively lightweight: about 54 kilograms (120 lbm)

(3) Capable of an air-launch start from windmilling conditions at altitude

(4) Capable of producing 2669 newtons (600 lbf) of thrust at sea-level static conditions

(5) Capable of producing 1557 newtons (350 lbf) of thrust at its cruise condition (flight Mach no., 0.8; and altitude, 6096 m (20 000 ft))

(6) Self-sufficient for a mission with a flight duration of 20 minutes.

More specifically, the engine should be designed to satisfy the operating characteristics, internal gas conditions, and other requirements summarized in table I.

A cross-sectional view of the design is shown in figure 1. It is an axial-flow turbojet engine with a four-stage compressor, an annular combustor, a single-stage turbine, and a fixed-area exhaust nozzle. Other features include:

(1) Compressor and turbine rotor disks cast integrally with their respective blading

(2) An integrally cast (360°, one-piece) turbine stator assembly

(3) An integrally cast compressor-inlet - front-main-bearing support

(4) An all-welded compressor-rotor-mainshaft assembly

(5) A simplified perforated combustor liner cooling system

(6) An inner annular wall of the liner cooling air passage formed by the engine mainshaft

(7) Simplex fuel nozzles in the combustor in lieu of the more costly and complex duplex or variable area nozzles

(8) An integrally cast turbine exhaust casing and rear main bearing housing

(9) An oil-mist bearing-lubrication system eliminating the need for an oil sump and oil pump

(10) A simplified fuel-pump - fuel control assembly

(11) A compressor-turbine rotor-mainshaft assembly simply supported through a soft mounted two-main-bearing system.

Design principles incorporated to reduce costs included one-piece castings with little or no machining, elimination of welded flanges, use of standard bolts, locking devices, and other parts, use of bolts or dowels instead of couplings, and the elimination of a recirculating lubrication system. These features, together with the selection, wherever possible, of lower cost materials and manufacturing processes contribute to the low production cost potential of the engine. Figure 2 shows the castings of major components used in the fabrication of the engine.

Air Inlet Section

The inlet housing was a one-piece aluminum (AMS 4214) sand casting having only two struts that connect an inner-housing – centerbody with the outer-shell housing. Figure 3(a) shows an inlet housing in the as-cast condition and a finished version having a minimum of machining operations. The annulus formed between the centerbody and the outer shell provided the flowpath for the air entering the compressor, and the centerbody served a dual function of housing the front engine main bearing and a small gearbox arrangement driven off the end of the compressor shaft. A more detailed view of the inlet section of figure 1 is presented in figure 3(b). Figure 3(c) is a photograph of the main components comprising the inlet-housing assembly. An access passage in one of the struts allowed a right-angle drive shaft (quill) from this gearbox to power an external fuel-pump/fuel-control assembly. The gearbox provides a 5:1 ratio for speed reduction from the end of the compressor shaft. Other access passages in the struts were used for front bearing lubrication and instrumentation. The two-strut arrangement for the inlet housing was selected primarily to satisfy vibration analysis requirements. Vibration analyses (ref. 10) for this design have shown that inlets having three or more struts might induce strong engine order interferences with the compressor rotor blades within the range of normal engine operating speeds (from about 20 000 to 38 000 rpm).

Compressor Section

The compressor section consisted of an all-welded rotor assembly, individual stator vanes, and compressor casing halves.

Rotor assembly. – The compressor rotor consisted of four integrally cast, blade - disk rotor stages and a rotor mainshaft. The number of airfoils in each rotor and stator stage of the compressor is given in table II. Each rotor stage and the mainshaft was precision investment cast from AMS 5355 (17-4 PH), a high strength stainless steel of relatively low cost and good machinability. Before machining, the castings were subjected to a double-solution treatment at 1311 K (1900° F). Figure 4 shows the compressor rotor components in the as-cast condition and after the required machining. The four individual rotor stages were circumferentially electron-beam welded at the hub flanges to form a one-piece drum, which served as the inner wall of the compressor airflow passage. Following a balancing procedure for the rotor mainshaft and the individual rotor stages, the mainshaft and the fourth-stage rotor were installed and aligned in a mounting fixture in preparation for the first electron-beam welding procedure. A complete circumferential weld was made joining the cone-shaped end of the mainshaft to the

downstream hub region of the fourth-stage rotor. Figure 5(a) shows the mainshaft and fourth-stage rotor installed in the mounting fixture after completion of this first welding procedure. The close-up photograph (fig. 5(b)) reveals the circumferential electron-beam weld bead, which attached these two components. Figure 5(c) shows the third-stage rotor along with the previously welded components installed in the mounting fixture, and figure 5(d) shows the mounting fixture with the compressor components installed in the welding facility ready for joining the third-stage rotor to the fourth-stage rotor. The other two stages were subsequently welded in a similar manner to complete the compressor rotor mainshaft assembly (fig. 5(e)). Following these welding operations, the assembly was subjected to an age-hardening process to bring it to condition H 1025. Final machining of the front bearing stub shaft and mainshaft seal surfaces was then accomplished along with blade tipping of the four rotor stages and attachment surfaces for bolting to the turbine rotor. Pertinent dimensions such as tip diameter, and airfoil chord, and span for the compressor rotor and stator stages are presented in table III. The average compressor-rotor tip diameter was about 20 centimeters (8 in.), and the nominal blade-tip to compressor-casing clearance at assembly was about 0.04 centimeter (0.016 in.).

Compressor stators and casing. - In keeping with the low-cost premise, the proposed design of the stator assembly called for two 180° integrally cast aluminum (AMS 4214) vane and shroud ring assemblies for each of the four compressor stages. The proposed compressor casing design called for two halves with the split lines in an axial direction with the halves being cast as integral units from the same aluminum material as the stator vanes. However, for these initial test engines, the compressor stator vanes were made adjustable to allow the optimization of vane setting angles. If subsequent engine assemblies were to be provided they could then incorporate the integrally cast split ring stators with vanes cast to the desired vane setting angle. The individual stator vanes used for the test engines were precision cast from the same material (17-4 PH) as that used for the compressor rotor stages. Figure 6 shows a cast vane from each of the four stages in the compressor section. The cast stub (stem) at one end of the vane was machined to provide threading for ease of mounting to the compressor casing with the lock nut shown. Flat surfaces were machined on the stem of the stator vanes to allow the vane angle setting to be adjusted.

The compressor casing designed for accepting these individual vanes was fabricated in two halves from mild steel (1020) heavy-walled tubing, with the split line in the axial direction. The left-hand portion of figure 7 shows the finish-machined and nickel-plated compressor casing halves with a single vane from each stage in the foreground; the right portion shows a set of compressor casing halves with all the stator vanes installed. At assembly, the clearances between the rotor drum and the tips of the stators were on the order of 0.04 centimeter (0.016 in.).

6

Combustor Section

This section of the engine consisted of a diffuser, the combustor assembly, and the outer housing. The annular combustor had a single side entry of primary and secondary air for burning and gas dilution in the combustion zone. An objective in the design of the combustor liners was to eliminate the need for the more expensively formed cooling-scoops or the plunged secondary air dilution holes. Figure 8 shows the combustor and outer housing assemblies along with the two surface-discharge igniters used to initiate the combustion process. Figure 9(a) presents an exploded view of all the components of the combustor assembly, and figures 9(b) and (c) provide downstream and upstream views of the combustor assembly. The snout or nosepiece formed a diffuser passage with the outer housing and provided acceptable airflow velocities for permitting a stable combustion process.

All components for the outer housing assembly were made from stainless-steel; the shell was fabricated from 20-gage (0.0953-cm (0.0375-in.)) AMS 5510 (AISI 321) sheet and shaped to design requirements through a hydroforming process, and the flanges from type 321 (AMS 5645) barstock. With the exception of the fuel manifold and the fuel nozzles, all other parts of the combustor assembly shown in figures 9(b) and (c) were fabricated from AMS 5536 (Hastelloy X) sheet metal. Both the inner and outer combustor liners were fabricated from commercially available 20-gage (0.0953-cm (0.0375-in.)) perforated sheet metal which was rolled to the desired cylindrical shape. The 0.32-centimeter (0.125-in.) diameter perforations were oriented in a simple hexagonal pattern, each hole being located 1.37 centimeters (0.541 in.) from the next hole; that is, each side of the haxagon formed by the perforations was 1.37 centimeters (0.541 in.) long. The hexagonal pattern of perforations included a hole at the center of the hexagon. A punch-press was used to incorporate large, circular and oblong flush holes into the outer liner for accommodating the primary and secondary airflow conditions for burning and gas dilution requirements. Additional air from the compressor (secondary air) flowed through the perforations in the sheet metal to provide the necessary cooling of the inner and outer combustor liners.

ASTM A-1 jet fuel was directed from a single tube to 12 simplex fuel nozzles that were arranged in a manifold. Each nozzle is set in an eight-bladed swirler, which promotes the proper mixing of air and fuel in the primary combustion zone. The simplex fuel nozzle, which is similar to those used in home oil-burning furnaces, was chosen because it is less expensive than the duplex or variable-area fuel nozzles in common usage. The results of references 11 and 12 indicated a satisfactory spray pattern for the conditions expected over the desired engine operating range.

A particular note of interest in this combustor design was the absence of an inner combustion housing wall. The compressorturbine – rotor shaft itself acted as one of

the boundaries for the secondary-air passage supplying cooling air to the perforated inner liner of the combustor assembly.

Similarly constructed combustor assemblies were tested in a combustor-component rig, and the results of these tests are reported in references 11 and 12. Results of tests such as these led to the final selection of hole patterns and hole sizes in the combustor liner for film cooling and dilution requirements. The open area of the primary and diluent holes for this combustor was increased by a factor of about 2 over that of the final version reported on in reference 12.

Turbine Section

This engine design used a single-stage axial-flow turbine, which consisted of a stator vane assembly and a bladed-rotor - disk assembly.

Turbine stator assembly. - The stator vane assembly consisted of 35 radially tapered airfoil vanes between two shroud rings. This assembly was precision invest-ment cast from AMS 5382 (Stellite 31) as an integral 360° casting. The outer shroud ring extended rearward past the trailing edge of the stator vanes about 2.5 centimeters (1 in.) and acted as the stationary shroud for the turbine rotor blades. Figure 10(a) shows an integral stator vane assembly in the as-cast condition and a fully machined version. The oblong or elliptically shaped hole in the extended portion of the outer shroud of the machined assembly allowed a single jet of air to impinge on the turbine blades for engine starting purposes. Cold-air performance tests were conducted on the turbine components, and the results are presented in references 13 and 14.

Turbine rotor. - The turbine rotor was an integrally cast rotor blade and disk as-sembly incorporating 57 radially tapered turbine blades. The material used in preci-sion investment casting the rotor assembly was IN-100 (AMS 5397), a high-temperature, high-strength nickel alloy. Figure 10(b) shows the rotor assembly in the as-cast condi-tion and as a fully machined component. The six through-holes shown on the machined turbine rotor assembly were used to bolt the turbine rotor to the end of the compressor-rotor - mainshaft assembly. Alignment was maintained by an interference fit between the bore of the rotor shaft and a piloting shoulder on the turbine rotor. Figure 5 shows the required bolts already in place at the end of the compressor rotor shaft. The bolts are used to attach the turbine rotor. Figure 11 shows a completed compressor-turbine rotor mainshaft assembly. In the machined condition the turbine rotor-tip diameter was 24.577 centimeters (9.676 in.), which allowed a blade tip-to-stator shroud clear-ance at assembly of about 0.040 centimeter (0.016 in.).

8

Exhaust Section

An enlarged view of both the turbine and exhaust sections (from fig. 1) is presented in figure 12(a). The exhaust section consisted of an exhaust duct (commonly referred to as an engine tailcone), a housing for the rear main bearing, and a jet-exhaust nozzle. All three components were fabricated from type 347 stainless steel. The exhaust duct was a one-piece casting (AMS 5362) that had the inner ducting (centerbody) connected to the outer ducting through three airfoil shaped radial support struts. This ducting provided the contoured passage for the jet exhaust and also acted as the supporting member for loads transmitted through the rear bearing. The bearing housing is also investment cast from AMS 5362 material as an integral piece. Figure 12(b) shows the exhaust duct and bearing housing in the as-cast version and as final machined parts. Figure 12(c) shows the associated hardware for the turbine and exhaust sections including necessary damper, spacers, etc., for mounting the bearing on the stub shaft of the turbine rotor. The outer race of the rear bearing was inserted in the bearing housing which, in turn, was bolted to the centerbody or inner cone of the exhaust duct. The forward bolting flange of the outer cone of the exhaust duct attaches to the turbine vane support ring and aft combustor housing flange, and provides support for the turbine stator through use of radial slots allowing for radial expansion of the stator. The exhaust nozzle which attached to the aft flange of the exhaust duct, was fabricated from type 347 stainless steel barstock and sheet and was of a conventional convergent design. The original nozzle length was sufficient to allow it to be machined or cut-back to optimize the nozzle throat area during preliminary testing.

Bearings, Lubrication, and Associated Cooling

The compressor-turbine rotor-mainshaft assembly (shown in fig. 11) was simply supported through a soft-mounted two-main-bearing system. The front bearing was located at the stub shaft at the stub shaft at the forward end of the compressor and was soft-mounted using a rubber O-ring to reduce vibration levels. This bearing was of a single row, ball type suitable for combined radial and thrust loads at speeds up to 40 000 rpm using an oil mist for lubrication. Additional front bearing specifications are provided in the following:

Size 205
Grade ABEC-5
Number of split inner rings 1
Bore, mm (in.) 25 (0.98)

Outside diameter, mm (in.). 52 (2.05)

Width, mm (in.). 15 (0.59)

Ball and race material . . . . .CVM 52100 steel

Number of balls 11

Ball diameter, mm (in.) 8 (0.3150)

Radial clearance, mm (in.). . . . . 0.0305 – 0.050 (0.0012 – 0.0020)

Pitch diameter, cm (in.) 3.7691 (1.4839)

Curvature, percent:

    fo 52

    fi 52

Inner ring shoulder diameter, cm (in.) 3.325 (1.309)

Cage[a]:

    Construction . . . . One piece, outer land riding

    Material   [b]4340 steel

    Silver plating thickness (all surfaces), ... 0.0127 – 0.0381 (0.0005 – 0.0015)
       mm (in.)

    Maximum unbalance after plating, gm-cm (oz-in.) 0.359 (0.005)

Surface finishes (rms), μm (μin.):

    Race grooves 0.1524 (6)

    Balls. . . . . 0.025 – 0.051 (1 – 2)

    Outer ring land (cage riding surface). 0.406 (16)

[a]Cage size was minimized to aid mist lubrication.

[b]Alternative material, silicon-iron bronze.

The rear bearing was located at the stub shaft of the turbine rotor and was soft mounted
using a metal-leaf spring to reduce vibration levels. This bearing was of a single-row,
cylindrical-roller type that was suitable for radial loads at speeds up to 40 000 rpm.
An oil mist lubricated the bearing. Additional information is provided in the following
table:

Size 240

Grade RBEC-5

Number of inner ring flanges 2

Bore, mm (in.) 20 (0.787)

Outside diameter, mm (in.). 47 (1.85)

Width, mm (in.). 14 (0.551)

Ball and race material . . . . CVM M-50 steel

Number of rollers 10

Radial clearance, mm (in.). . . . . 0.0456 – 0.0559 (0.0018 – 0.0022)

Roller size, mm (in.) . . . . 7 by 7 (0.28 by 0.28)

Cage[a]:

    Construction. . . . . One piece, inner land riding

    Material . . . . 4340 steel

    Silver plating thickness (all surfaces, ... 0.0127 - 0.0381 (0.0005 - 0.0015)
      mm (in.)

    Maximum unbalance after plating, gm-cm (oz-in.) 0.359 (0.005)

[a]Cage size was minimized to aid most lubrication.

Schematic diagrams of the bearing-mount designs for both the front and rear bearing are shown in figure 13.

    Figure 14(a) presents a schematic diagram of the bearing lubrication-cooling systems. Each bearing was serviced by a separate oil-mist generator with a capacity of up to 120 grams (4 fluid oz) of oil (conforming to MIL-L-23699) which was sufficient for about $2\frac{1}{2}$ hours of engine operation at rated conditions. Figure 14(b) shows these oil-mist generators along with associated bearing lubrication and cooling-air lines. Bleed air from the compressor discharge was piped to the generators at the rear of the engine for producing the lubricating oil mist. Mist oil supplied from one generator was directed to the front of the engine through one of the inlet housing struts to the gear box and main-bearing housing cavity. During normal engine operation, a positive pressure differential existed between the bearing housing cavity on one side of the main bearing and the front side of the compressor rotor at the other side of the bearing. This pressure differential forced the oil mist onto the main bearing proper or through the spaces between the bearing races. Any excess oil was harmlessly discharged into the compressor inlet area.

    Mist from the other generator was directed through tubing in a strut of the exhaust ducting to discharge in the rear bearing housing cavity for lubricating the roller bearing. Bleed air from a separate line from the compressor's second stage was used to provide rear bearing cooling. Appropriate vent lines from the rear bearing cavity region through the struts in the exhaust ducting to an external location on the engine were provided for overboard bleed of the cooling air and oil-mist discharge. Since the front bearing was located in a much cooler operating region, supplemental cooling was not required there.

Fuel Control

    The basic concept and principles for operation of the fuel control are discussed in detail in references 6 to 15. Briefly, the simplified hydromechanical approach

11

consisted of a series-parallel combination of orifices that were used to generate the desired control limits. The concept was based on the assumption that the maximum and minimum fuel schedules for acceleration and deceleration limits can be described as linear functions of corrected engine parameters. The fuel control schematic diagram of figure 15 (taken from ref. 8) is representative and descriptive of the mechanism used for the fuel control on this engine. Appropriate taps from the compressor inlet P_2 and compressor discharge P_3 supplied the required pressures for proper operation of the fuel control as illustrated in this figure. Fuel is provided to the fuel control by a small gear pump housed within the fuel control body. Power is provided by a quall shaft driven by the engine rotor mainshaft through a 5:1 reduction right angle gear mesh. The fuel control assembly bolted directly to the top of the inlet housing.

Engine Assembly

The photographs of figure 16 show the engine in various stages during a normal assembly procedure. The assembly stand was designed to facilitate taking necessary measurements, including various dimensions, clearances, and runouts during the assembly procedure. Figure 16(a) shows the compressor-turbine rotor mainshaft assembly being lowered to align with its mating part, the bearing housing of the inlet section. Before this assembly procedure, the compressor-turbine rotor mainshaft assembly was dynamically balanced to within 0.359 gram-centimeters (0.005 oz-in.) at the balance planes of each bearing location. Figure 16(b) shows the compressor casing halves being installed around the compressor rotor mainshaft and attached to the inlet housing. Next, in figure 16(c) the combustor and its housing are shown being attached to the compressor casing halves. Actually, one casing half is shown removed to check the clearances between the compressor rotor blade tips and the casing. Note also the turbine rotor has now been removed from the mainshaft to allow the installation of the turbine stator ring assembly. Figure 16 (d) shows the engine with both the turbine stator and turbine rotor assembled in place. In figure 16(e) the rear bearing system and exhaust ducting have been added to complete the assembly steps. After this procedure, the engine was removed from the vertical stand and mounted horizontally on a test stand to complete all the other necessary assembly procedures before installation in a test cell. On the test stand, the engine was supported at the front through a pivoting trunnion that was attached to mounting bosses on the inlet housing Except for a pivoting action in the plane of the engine's axis, the engine was otherwise fixed at this location. Additional support was provided in the rear of the engine by a pin and yoke that attached to the mating flanges of the combustor housing and the exhaust duct. This pin and yoke provided support in both the vertical and transverse direction, and allowed for thermal

expansion along the engine's axis. With the addition of such items as the exhaust jet nozzle, oil-mist generators and associated piping, cooling air lines, research and operational instrumentation, and an inlet bellmouth section, the engine assembly is ready for installation in a NASA-Lewis sea-level static test cell site (fig. 17(a)). For comparison, figure 17(b) shows the basic engine with only the bare essentials before shipment to the Naval Weapons Center. The engine's major diameter (29.2 cm (11.5 in.)) occurred at the combustor housing and the length of the engine from the nose cone to the lip of the exhaust nozzle was 96.5 centimeters (38 in.). The weight of the basic engine (without oil misters, extraneous tubing or piping, etc.) was about 59 kilograms (130 lbm). A decrease in overall weight of at least 4.5 kilograms (10 lbm) can be expected when aluminum is substituted for the iron alloy presently being used for the compressor casings and stator vanes.

TEST FACILITIES

Two Lewis facilities were used to conduct the programs for the test engines. All sea-level static testing was conducted in the special projects laboratory and all simulated flight testing was conducted in the propulsion systems laboratory. Figure 18 shows an engine installed in the SPL facility. Although the altitude chamber of PSL was capable of simulating altitudes from near sea level up to 24 380 meters (80 000 ft) and flight Mach numbers up to 3.0, the full capacity of this facility was not required for this investigation.

INSTRUMENTATION

Research and operational instrumentation was provided on the test engine to determine the engine performance characteristics, and to assure safe operating conditions. Figure 19 is a schematic of the engine showing the locations of various engine stations where pressure or temperature measurements were made to determine flow conditions of the main gas stream. The symbols shown by the station numbers refer to the type of measurements made there. All temperature measurements were made with Chromel-Alumel thermocouples; static pressures were obtained from wall taps; and total pressures from probes or rakes inserted into the air or gas stream. Other important measurements included bearing temperatures, engine speed, fuel flow, engine thrust, and vibrational characteristics. The bearing temperatures were obtained from thermocouples attached to the outer race; the engine speed signal was obtained through a magnetic pickup; fuel flow was determined from turbine flowmeters; thrust readings

were obtained through a load cell; and vibrational data were obtained through accelerometers and a proximity probe. Two accelerometers were located at both the front and the rear of the engine and were positioned to indicate the vibration levels in both the vertical and horizontal direction. The proximity probe was mounted directly over a retaining ring which houses the outer race of the front bearing in order to provide an indication of the shaft displacement. Most of the measurements for testing information were recorded on the Central Automatic Digital Data Encoder (CADDE) system. Temperatures, fuel flows, engine speed, etc., were recorded as voltage outputs through the Automatic Voltage Digitizer (AVD) system, and pressures were recorded through the Digital Automatic Multiple Pressure Recording (DAMPR) system. The data were then processed in a digital computer. A detailed description of the CADDE system is given in reference 16. A number of duplicate measurements were also recorded on strip chart recorders to provide a continuous record during operation.

DISCUSSION

Over a period of approximately 2 years, four engine assemblies were completed and tested at Lewis. Engine testing was conducted at both sea-level static and simulated altitude conditions. Engine speeds as high as 38 000 rpm (representing an overspeed condition of about 8 percent) and turbine-inlet temperatures as high as 1255 K (1800° F) were investigated at sea-level static conditions. Testing at simulated flight conditions included Mach numbers as high as 1.2 and altitudes as high as 9144 meters (30 000 ft). Upon successful completion of all required testing, two engines were delivered to the Naval Weapons Center for their own demonstration testing purposes. The purpose of this section is to discuss some operating characteristics peculiar to these engines along with some general observations as a result of the testing. The engine performance characteristics obtained from testing at both sea-level static and simulated flight conditions will be presented as Part II of this report.

Engine Starting

For achieving an engine start at sea-level static conditions, initial rotation of the compressor-turbine rotor was accomplished by a single jet of air impinging on the turbine rotor blades. Air, from a laboratory supply of about 965 kilonewtons per square meter (140 psia) was used to accelerate the rotor to a speed of about 7000 rpm, which resulted in an airflow through the engine of about 0.50 kilogram per second (1.1 lbm/ sec). After the surface-discharge igniters were activated, jet A-1 fuel was supplied to

14

the combustor at a flow rate of about 0.021 kilogram per second (0.047 lbm/sec) to achieve the correct conditions for a normal start. For these conditions a minimum throttle position was preset so that the engine would accelerate automatically to a speed of about 23 000 rpm (65 percent of rated engine speed). Early sea-level static operation with the facility fuel system along with bench tests of the fuel control helped establish initial fuel-control adjustments. Subsequent engine tests with the fuel control allowed the optimization of settings to provide the best starting and operating characteristics. At simulated flight conditions the ram air supplied to the engine inlet was used to windmill the engine to adequate speeds to accommodate engine start. Windmilling speeds resulting from simulated flight conditions necessitated appropriate adjustments in required fuel flow rate for proper engine starting conditions.

The curves of figure 20 present typical engine startup characteristics at sea-level static conditions. The curves present temperatures at stations 5 and 6, engine speed and fuel flow as functions of time.

Full-scale Engine Operation

Compressor. - Initial full-scale engine testing was conducted to determine the optimum setting angles for the adjustable stator vanes in the four compressor stages of this engine design. Results of these tests revealed a disturbingly low compressor efficiency, and, regardless of how the stator vanes were adjusted, it appeared that the efficiency could not be greatly improved. Therefore, several modifications were made to the compressor's components in an attempt to improve its efficiency. Without elaborating in any detail, the following is a summary of modifications that were made:

(1) The stator vanes and blades were chem-milled to reduce the vane and blade thickness and decrease the leading and trailing edge radii.

(2) The compressor rotor blades were twisted to alter blade setting angle. Obviously, it was impossible to effect a change in the setting angle at or near the blade-to-hub junction of the integrally cast rotors, so most of the blade setting angle change occurred above the midspan of the blades.

(3) The vane-to-stem junctions of the stator vanes were machined to reduce the root radius and provide a smoother gas flow path along the internal surface of the compressor casing.

(4) Rotor blades were reshaped (by bending) to alter blade camber angles in the leading and trailing edge regions. Most of the change occurred in the outer span region of the blades for the same reason as that discussed in item (2).

(5) The clearances between rotor blade tips and compressor casing were reduced.

15

(6) Circumferential grooves in the compressor casing were machined over rotor blade tips to increase stall margin.

(7) The frontal area to the compressor inlet was increased.
None of these modifications significantly improved the compressor efficiency, and it was concluded that only major redesign could accomplish the desired results. (The procedures used for producing the geometrical changes mentioned in items (1), (2), and (4) are discussed in detail in ref. 17.) Because Lewis was required to meet a deadline, such an effort was not feasible and therefore engine testing continued to determine its overall performance capabilities, primarily its thrust potential.

Turbine. - During preliminary testing, it was determined that the turbine stator throat area should be increased by about 10 percent to better match the output of the compressor. As received, the throat area of the integrally cast turbine stator assemblies was about 5 percent undersize, so that the desired throat area was only 5 percent above the original design value. A special tool shaped to the contour of the pressure surface of the vane trailing edge region was used in conjunction with a compression head of a tensile testing machine to forcefully open the throat area to the desired value. This process usually resulted in a minute crack near the filleted region of the vane trailing edge at both the inner and outer rings. Center punch marks were placed at the end of the cracks to monitor crack propagation at periodic intervals of engine operation. No significant crack propagation was detected in this region, but cracks in the leading edge of a few vanes, at about the midspan location, did initiate after testing at the very high average turbine-inlet temperatures (about 1255 K (1800° F)). According to component tests on combustors in reference 12, the pattern factor obtained for similar conditions could have produced maximum local temperatures as high as 1439 K (2130° F). Figure 21 is a closeup of the leading edge of a turbine stator vane revealing a crack that has initiated and propagated for a distance of about 0.86 centimeter (0.34 in.).

After about 35 hours of varied and intensive testing on one engine assembly, a turbine rotor blade failed. The blade had fractured at a span dimension of about 0.64 centimeter ($\frac{1}{4}$ in.) above the blade root (integral blade-to-disk joint). An inspection of the turbine rotor revealed that five other blades had chordwise cracks in the trailing edge region at about the same span location. Figure 22(a) shows the turbine rotor with the missing blade and the cracked blades. Figure 22(b), a closeup of the trailing edge of blade 21, reveals the crack that was already about 0.95 centimeter ($\frac{3}{8}$ in.) long. A microscopic inspection of the failed surfaces of these blades indicated that the failures were more than likely a result of high-cycle fatigue. The vibration analysis conducted for this engine design, however, did not indicate any potentially critical resonance problems with respect to the interference diagrams generated for the turbine blades over the range of engine speeds for testing conditions. The interference diagram

(fig. 23) shows the fundamental natural frequencies of the turbine blade for the first bending and first torsional modes along with curves of selected engine-order excitation frequencies superimposed. Besides the 1 and 2 per revolution engine orders normally generated by the engine, other engine orders of significant interest would be 3 and 35 since there were three struts just downstream of the turbine blades and 35 turbine stator vanes just upstream of the turbine rotor blades.

A hologram-vibration study was made on an individual blade and on an entire turbine rotor wheel; the results are presented in reference 17. It is suspected that a 6-engine-order excitation may have existed during operation of the engine. This excitation could possibly have been generated by some harmonic interaction of the three downstream struts in the exhaust duct. As shown in the interference diagram, the 6-engine-order curve intersects the turbine blade first mode bending curve at about 31 500 rpm, where an appreciable amount of engine testing was conducted. The unknown aspects of the failure mode indicate the need for rigorous analysis and possibly engine developmental testing before new engines incorporating undamped integrally cast rotors are certified for long-time service or man-rated applications.

Exhaust nozzle. - Tests were conducted to determine the optimum, safe size of fixed-area exhaust nozzle to be used for obtaining test data. The engine was operated over a range of engine speeds with three different exhaust nozzles having areas of 265, 245, and 239 square centimeters (41, 38, and 37 in.^{2}). The plot of compressor pressure ratio as a function of compressor weight flow in figure 24 illustrates the engine's operating lines for the three exhaust nozzles used. The stall line plotted in this figure was determined from previous testing of this particular compressor in a compressor test rig before installation in this engine. The dashed portion of the curve represents an extrapolation of established data. No attempt was made to determine the actual engine stall line during engine operation, but, generally speaking, the compressor stall line is a fair indicator of the stall region for engine operation. As can be seen from the operating curve for the 239-square-centimeter (37-in.^{2}) nozzle (fig. 24), the stall margin is quite small (about 2 to 3 percent), but the engine did not experience any surge or stall problems during the steady-state operational testing. Later testing, where rapid movement of the throttle was required (snap accelerations) did present some stall problems but even these were alleviated by adjustments in the fuel control. During the progress of this program, the Naval Weapons Center requested Lewis to increase the engine's potential thrust output (by about 222 N (50 lbf)) over that of its original rating of 2670 newtons (600 lbf). Because the original engine design was considered to be conservative from the standpoint of turbine-inlet temperature and rotor stresses, it did appear possible that the engine speed and turbine-inlet temperature could be safely increased to give a higher thrust output. Increasing the thrust capability would require the use of the smallest (239 cm^2 (37 in.^{2})) exhaust nozzle even

though the stall margin was considered minimal at sea-level conditions. It was expected, however, that the ram pressures existing at flight conditions would improve the surge margin over that of sea-level-static tests for a given size of exhaust nozzle area.

Combustor. - Testing over a wide range of operational conditions resulted in some noticeable warpage of the perforated sheet metal combustor liners in this engine. The warpage was not considered unusual though and had no apparent effect on engine performance characteristics. Operational testing also resulted in carbon deposits being formed on the fuel nozzles and on the surface of the combustor firewall as shown in figure 25. It is suspected that most of the carbon buildup that was formed resulted from operation at low or idle engine speeds where the combustion efficiency is generally very low. This was not abnormal, but extended operation at low engine speeds should be avoided to minimize carbon deposits. Despite the carbon buildup, there was no apparent impairment of engine starting or performance characteristics over the period of testing.

Vibration characteristics. - Engine vibration levels were monitored for all testing with four accelerometers and the shaft orbit detector (proximity probe) mentioned in the INSTRUMENTATION section. Unexpectedly high vibration levels, experienced during the early stages of the full-scale engine tests, necessitated a change in the design of the front and rear bearing mounts. The bearing mount stiffness rates were higher than had been estimated and thereby contributed to the adverse vibrational condition.

A vibration analysis had been conducted on the rotor shaft during the original engine design phase to examine rotor shaft critical speeds for the first three modes (cylindrical, conical, and bent shaft, respectively), as they would be influenced by shaft flexibility and by both bearing and bearing mount flexibility. The calculated values for the first and second rigid-body critical speeds as a function of bearing support stiffness are shown in figure 26. The design objective was to maintain the stiffness, or spring rate, at a level low enough for the expected critical speeds of the first and second modes to be appreciably below the expected operational speeds. It was anticipated that extended operation of the engine would occur between the speeds of 23 000 and 39 000 rpm. A spring rate of 70 000 newtons per centimeter (40 000 lb/in.) was established as the required value for both the front and rear bearing mounting arrangements. For this stiffness value it was estimated that the rotor critical speeds for the first two modes would be about 7000 and 14 000 rpm, and for the third mode to be about 270 percent of the rated engine speed (and therefore not of any real concern).

The original bearing mount designs (both front and rear) used a metal spring which resembled a collar. Eight lands were located on the inner diameter of the collar, and eight more lands were placed on the outer diamter so that they were spaced between the lands on the inner diameter. During the initial full-scale engine tests, high vibration and shaft displacement level led to the conclusion that the spring rates for this metal collar design were higher than originally estimated. After a series of trial and

error modifications, the bearing mount designs were changed to the final versions shown earlier in figure 13. The rear bearing-mount design still retained the metal collar concept, but the number of lands on both the inner and outer diameter were reduced from eight to four as shown in figure 27. For the front bearing mounting system, the final design used Vyton rubber O-rings to reduce the mounting stiffness and at the same time provide additional damping. The 0.24-centimeter (3/32-in.) diameter (thickness) O-rings were installed in grooves having the geometry shown in figure 28; this resulted in a radial compression (preloading on the O-rings) of about 12 percent.

Subsequent engine operation with these final design versions for the front and rear bearing mounts revealed a drastic reduction in the vibration indications to acceptable levels. Except for a few sporadic peaks, the vibration levels were contained in the region of from 2 to 7 g's. Figure 29 illustrates typical vibration levels at sea-level-static conditions for the range of engine speeds investigated. The typical relative displacement of the rotor shaft, as detected by the proximity probe, is illustrated by figure 30 for the range of operating speeds investigated. The shaft displacement increased gradually for an increase in engine speed to a maximum value of about 12.7 micrometers (0.5 mil), peak to peak, at the highest operating speed (105 percent of rated).

SUMMARY OF RESULTS

The four engines assembled during this investigation were subjected to a wide range of simulated testing conditions totaling 157 hours. Tests were conducted at both sea-level-static and simulated flight conditions including average turbine-inlet temperatures as high as 1255 K (1800° F) and engine speeds as high as 38 000 rpm. Preliminary tests conducted on the engine revealed some early developmental problems that could normally be expected in such an experimental venture. Efforts to quickly improve the low compressor efficiencies exhibited in early tests were only partially successful. It was concluded that only a redesign could completely correct this deficiency.

The method used to open the turbine stator throat area proved effective with subsequent testing showing improved matching characteristics between the compressor and turbine. Despite the resulting short cracks in the vane trailing-edge fillet regions at the shroud rings, no propagation of these cracks was observed after subsequent testing. The oil-mist bearing lubrication system successfully performed its intended function. At maximum operating conditions the bearing temperatures were steady at an acceptable level of about 367 and 461 K (200° and 370° F) for the front and rear bearings, respectively. After the bearing mount systems were redesigned (the four-land metal spring (collar design) for the rear and the 0.24-cm (3/32-in.) diam O-ring design for the

front), the engine operated within acceptable vibration levels. This soft mounting O-ring concept appears to have excellent potential for optimizing mount stiffness for minimum bearing loading.

Despite the undetermined cause for a turbine rotor blade failure after 30 hours of varied operation, the integrally cast compressor and turbine-blade - disk assemblies were regarded as structurally sound and performed exceptionally well for their intended short-life application.

Lewis Research Center,
    National Aeronautics and Space Administration,
        Cleveland, Ohio, February 9, 1976,
           505-04.

REFERENCES

1. Roelke, Richard J.; and Stewart, Warner L.: Turbojet and Turbofan Cycle Considerations and Engine Configuration for Application in Lightweight Aircraft. NASA TM X-1624, 1968.

2. Kraft, Gerald A.; and Miller, Brent A.: Off-Design Theoretical Performance of Three Turbofan Engines for Light Subsonic Aircraft. NASA TM X-52469, 1968.

3. Dugan, James F. Jr.: Theoretical Performance of Turbojet Engine for Light Subsonic Aircraft. NASA TM X-52538, 1969.

4. Cummings, Robert L.; and Gold, Harold: Concepts for Cost Reduction in Turbine Engines for General Aviation. NASA TM X-52951, 1971.

5. Cummings, Robert L : Experience with Low Cost Engines. NASA TM X-68085, 1972.

6. Seldner, Kurt; and Gold, Harold: Computer and Engine Performance Study of a Generalized Parameter Fuel Control for Jet Engines. NASA TN D-5871, 1970.

7. Batterton, Peter G.; and Gold, Harold: Experimental Test Results of a Generalized-Parameter Fuel Control. NASA TN D-7198, 1973.

8. Gold, H.: A Simplified Fuel Control Approach for Low Cost Aircraft Gas Turbines. SAE Paper 730388, Apr. 1973.

9. Ellis, C.; et al.: Design of the NASA Simplified Turbojet Engine C. CW-WR-69-057, Curtiss-Wright Crop. (NAS-3-12423), 1969.

20

10. Ellis, C.; Leto, A.; and Schaefer, R.: Compilation of Preliminary Design Data on Ordnance Engine. CW-WR-70-074, Curtiss-Wright Corp. (NAS-3-12423; Task 1010), 1970.

11. Fear, James S.: Performance of a Small Annular Turbojet Combustor Designed for Low Cost. NASA TM X-2476, 1972.

12. Fear, James S.: Performance of an Annular Combustor Designed for a Low Cost Turbojet Engine. NASA TM X-2857, 1973.

13. Kofskey, Milton G.; Roelke, Richard J.; and Haas, Jeffrey E.: Turbine for a Low-Cost Turbojet Engine. I - Design and Cold Air Performance. NASA TN D-7625, 1974.

14. Kofskey, Milton G.; Nusbaum, William J.; and Haas, Jeffrey E.: Turbine for Ordnance Turbojet Engine. II - Cold Air Performance with Opened Stator. NASA TN D-7626, 1974.

15. Seldner, Kurt; et al.: Performance and Control Study of a Low-Pressure-Ratio Turbojet Engine for a Drone Aircraft. NASA TM X-2537, 1972.

16. Central Automatic Data Processing System. NACA TN 4212, 1958.

17. Dengler, Robert P.: Experience with Integrally-Cast Compressor and Turbine Components for a Small, Low-Cost, Expendable-Type Turbojet Engine. NASA TM X-71782, 1975.

TABLE I. – ENGINE DESIGN VALUES FOR OPERATING CHARACTERISTICS AND INTERNAL GAS CONDITIONS

Condition	Sea level static	Cruise
Altitude, m (ft)	0 (0)	6096 (20 000)
Mach number	0 (0)	0.8
Ambient temperature, K (^{O}F)	288 (59)	249 (-12)
Power setting	Max.	Cruise
Speed, rpm	35 170	34 700
Inlet pressure ratio	0.95	0.99
Compressor:		
Airflow, kg/sec (lbm/sec)	4.387 (9.672)	3.24 (7.14)
Inlet temperature, K (^{O}F)	288 (59)	281 (45)
Outlet temperature, K (^{O}F)	455 (359)	439 (331)
Inlet pressure, N/m^2 (psia)	96 530 (14.0)	70 330 (10.2)
Pressure ratio	4.0	4.0
Adiabatic efficiency	0.83	0.85
Outlet pressure, N/m^2 (psia)	384 740 (55.8)	281 320 (40.8)
Combustor:		
Adiabatic efficiency	0.96	0.96
Outlet temperature, K (^{O}F)	1119 (1555)	1089 (1500)
Outlet pressure, N/m^2 (psia)	360 610 (52.3)	263 390 (38.2)
Heating value, J/kg (Btu/lbm)	4.33×10^7 (18 640)	4.33×10^7 (18 640)
Burner pressure ratio	0.937	0.937
Fuel–air ratio	0.0183	0.0172
Turbine:		
Adiabatic efficiency	0.88	0.88
Pressure ratio	1.881	1.854
Mass flow, kg/sec (lbm/sec)	4.468 (9.849)	3.296 (7.267)
Outlet temperature, K (^{O}F)	979 (1302)	954 (1258)
Outlet pressure, N/m^2 (psia)	191 680 (27.8)	142 040 (20.6)
Nozzle:		
Nozzle pressure ratio	1.891	3.048
Nozzle area, m^2 (ft^2)	0.0179 (0.193)	0.0179 (0.193)
Thrust coefficient	0.99	0.99
Performance:		
Net thrust, N (lbf)	2543 (571.8)	1562 (351.2)
Specific fuel consumption	1.114	1.300
Specific thrust, N·sec/kg (lbf-sec/lbm)	579.7 (59.12)	482.1 (49.19)

TABLE II. – AIRFOIL COMPLEMENT

FOR COMPRESSOR AND

TURBINE STAGES

Component	Stage			
	1	2	3	4
Compressor rotor	23	29	36	38
Compressor stator	28	36	42	42
Turbine rotor	57	--	--	--
Turbine stator	35	--	--	--

TABLE III. – DESIGN DIMENSIONS OF VARIOUS AIRFOILS AT HUB AND TIP SECTIONS

[All dimensions are in cm (in.).]

Stage	Hub				Tip				Span at midchord	Tip diameter at midchord
	Maximum thickness	Chord length	Leading edge radius	Trailing edge radius	Maximum thickness	Chord length	Leading edge radius	Trailing edge radius		
Compressor rotor										
1	0.267 (0.105)	3.193 (1.257)	0.036 (0.014)	0.048 (0.019)	0.130 (0.051)	3.218 (1.267)	0.018 (0.007)	0.018 (0.007)	4.567 (1.798)	19.76 (7.78)
2	0.330 (0.130)	2.365 (0.931)	0.043 (0.017)	0.066 (0.026)	0.102 (0.040)	2.372 (0.934)	0.018 (0.007)	0.018 (0.007)	3.426 (1.349)	19.96 (7.86)
3	0.183 (0.072)	1.938 (0.763)	0.030 (0.012)	0.041 (0.016)	0.091 (0.036)	1.946 (0.766)	0.018 (0.007)	0.018 (0.007)	2.522 (0.993)	20.34 (8.01)
4	0.163 (0.064)	1.872 (0.737)	0.023 (0.009)	0.025 (0.010)	0.094 (0.037)	1.875 (0.738)	0.018 (0.007)	0.018 (0.007)	1.946 (0.766)	20.65 (8.13)
Compressor stator										
1	0.112 (0.044)	1.989 (0.783)	0.018 (0.007)	0.018 (0.007)	0.224 (0.088)	2.54 (1.000)	0.038 (0.015)	0.028 (0.011)	3.795 (1.494)	19.81 (7.80)
2	0.112 (0.044)	1.781 (0.701)	0.018 (0.007)	0.018 (0.007)	0.185 (0.073)	1.999 (0.787)	0.028 (0.011)	0.023 (0.009)	2.741 (1.079)	20.24 (7.97)
3	0.127 (0.050)	1.654 (0.651)	0.018 (0.007)	0.018 (0.007)	0.178 (0.070)	1.651 (0.650)	0.023 (0.009)	0.023 (0.009)	2.207 (0.869)	20.57 (8.10)
4	0.127 (0.050)	1.676 (0.660)	0.018 (0.007)	0.018 (0.007)	0.180 (0.071)	1.676 (0.660)	0.023 (0.009)	0.023 (0.009)	1.778 (0.700)	20.85 (8.21)
Turbine rotor										
1	0.363 (0.143)	2.121 (0.835)	0.079 (0.031)	0.038 (0.015)	0.160 (0.063)	1.857 (0.731)	0.051 (0.020)	0.038 (0.015)	4.191 (1.65)	24.59 (9.68)
Turbine stator										
1	0.414 (0.163)	2.908 (1.145)	0.094 (0.037)	0.038 (0.015)	3.993 (1.572)	2.192 (0.863)	0.094 (0.037)	0.038 (0.015)	3.962 (1.560)	24.49 (9.64)

24
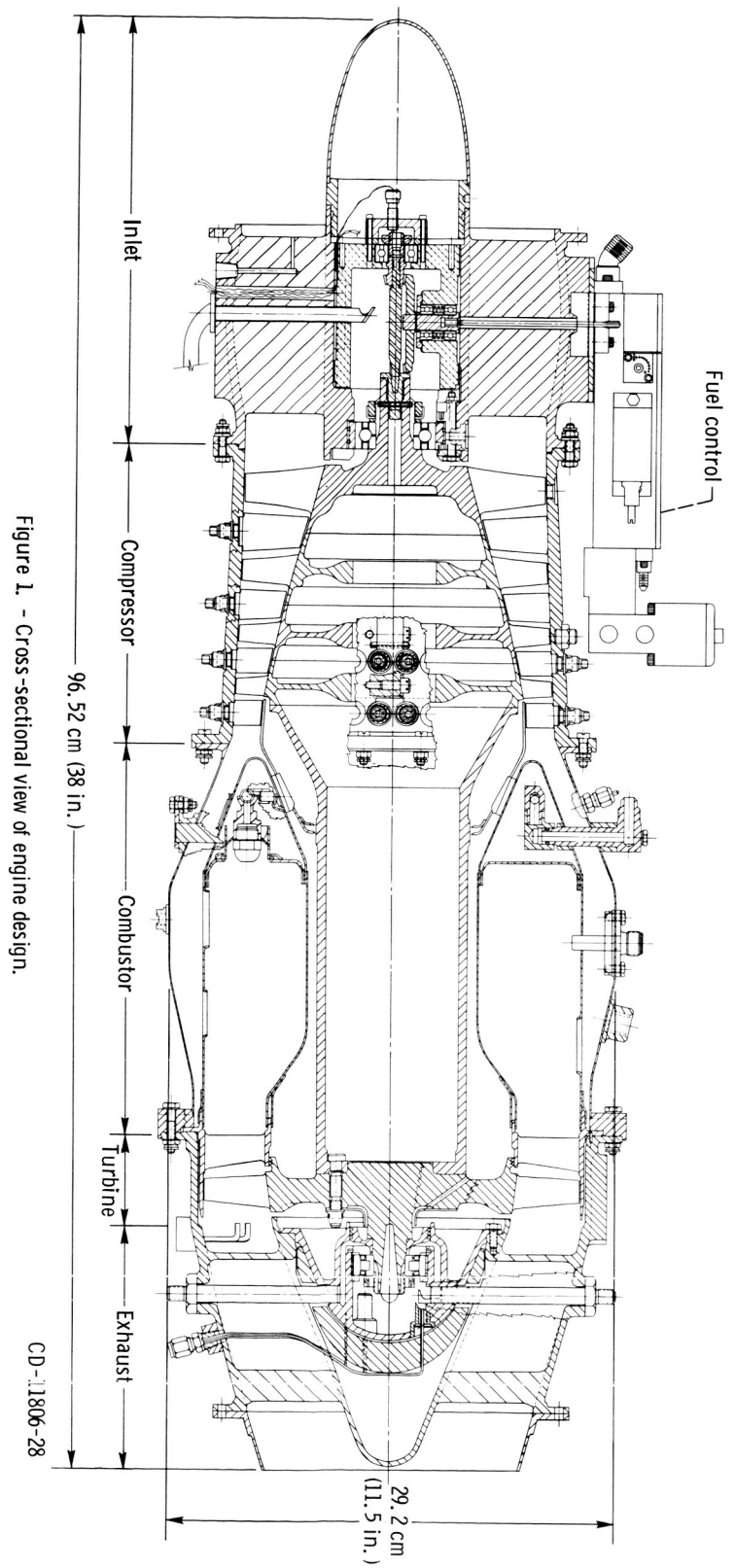
Figure 1. - Cross-sectional view of engine design.

Inlet

Compressor

Combustor

Turbine

Exhaust

Fuel control

96.52 cm (38 in.)

29.2 cm (11.5 in.)

CD-11806-28
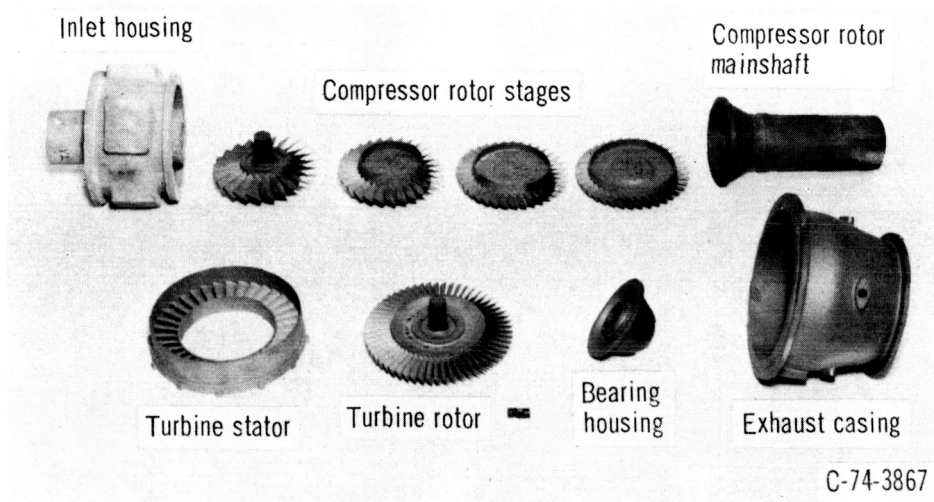
Figure 2. – Castings of major components for small-engine design.
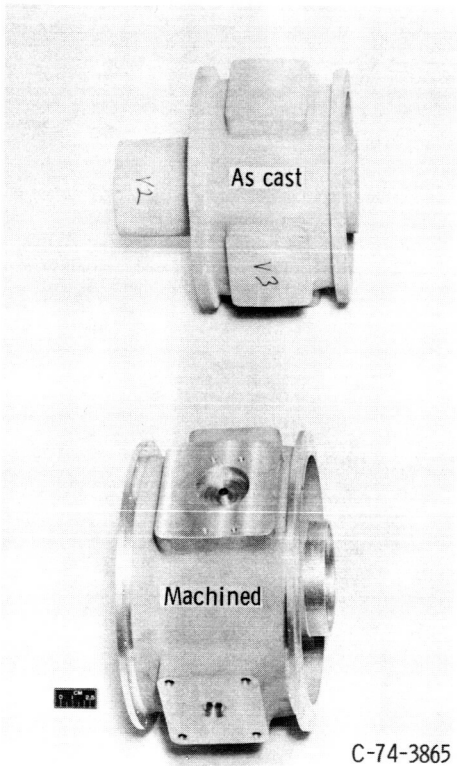
(a) Inlet housing in as-cast and machined conditions.

C-74-3865
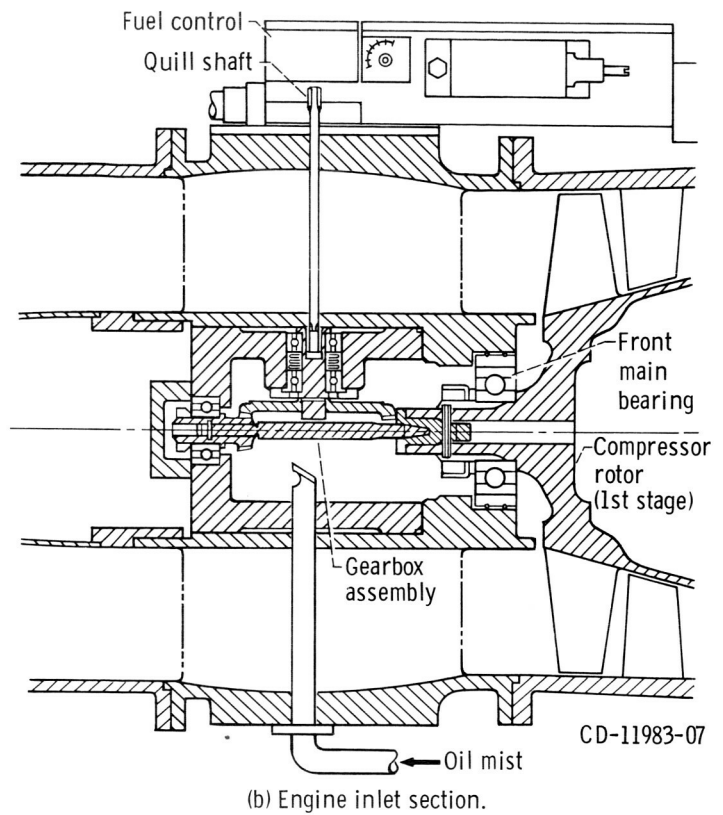
(b) Engine inlet section.

CD-11983-07
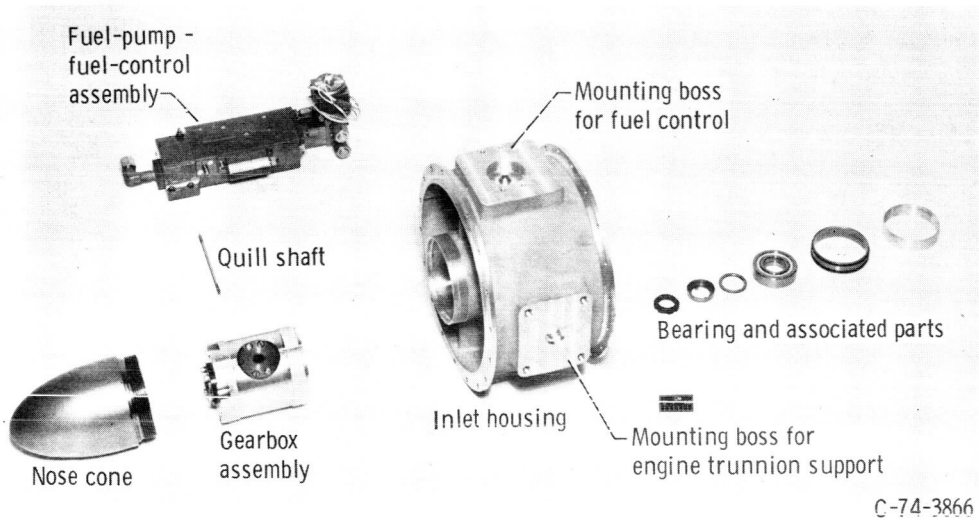
(c) Main components comprising inlet-housing assembly.

C-74-3866

Figure 3. - Air inlet section components.

Machined components

1st stage   2nd stage   3rd stage   4th stage   Mainshaft

As-cast components

C-74-3874
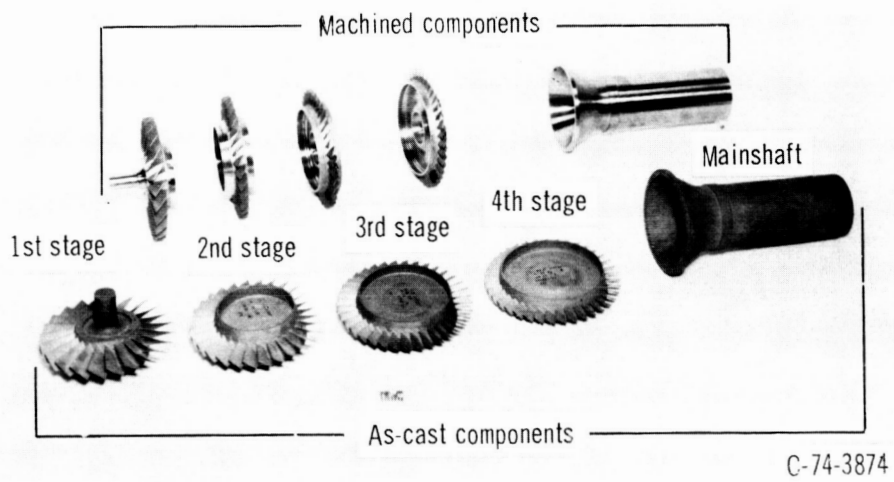
Figure 4. - Compressor rotor components in as-cast and machined conditions.
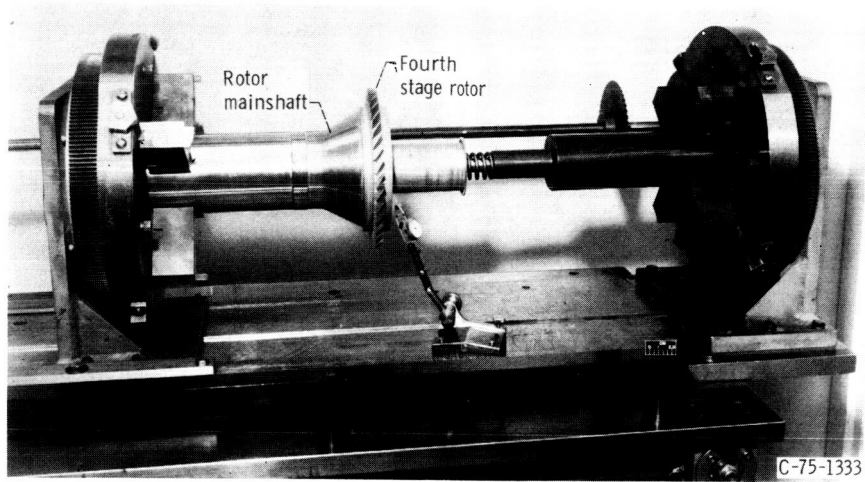
(a) Compressor mainshaft and fourth stage rotor installed in welding fixture.
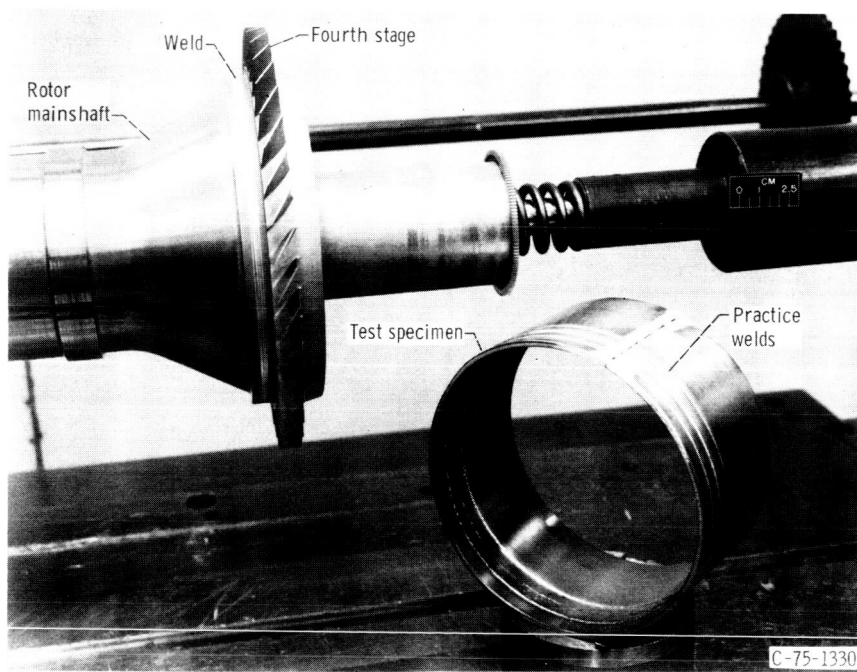
(b) Electron beam weld joining rotor mainshaft to compressor fourth stage rotor.

Figure 5. - Compressor welding steps.
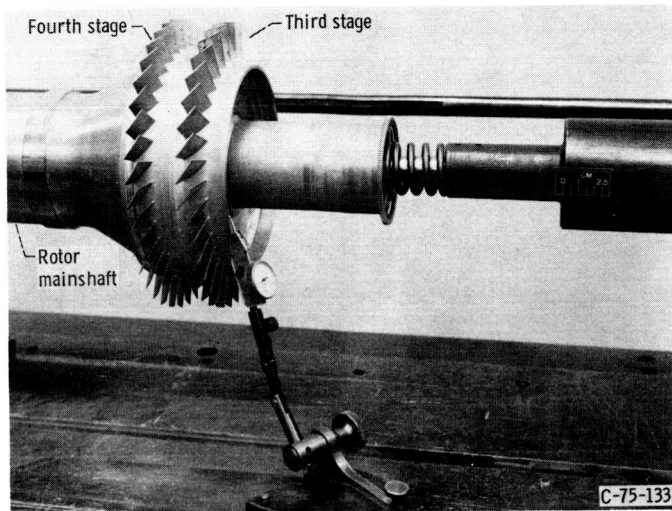
(c) Third stage rotor installed in fixture for welding to fourth stage rotor.
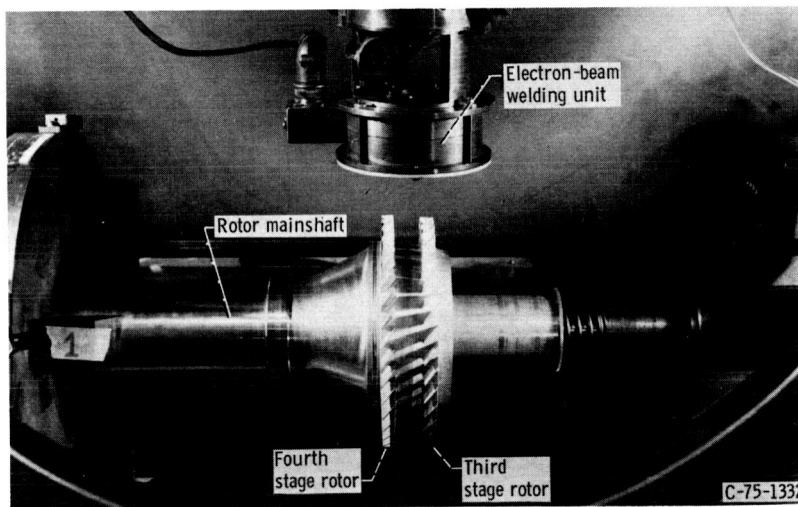
(d) Compressor-rotor components installed in welding facility.
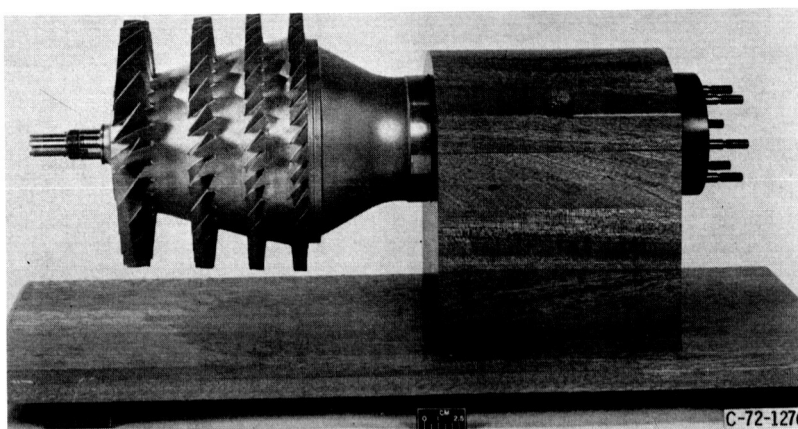
(e) All-welded compressor-rotor assembly.

Figure 5. - Concluded.
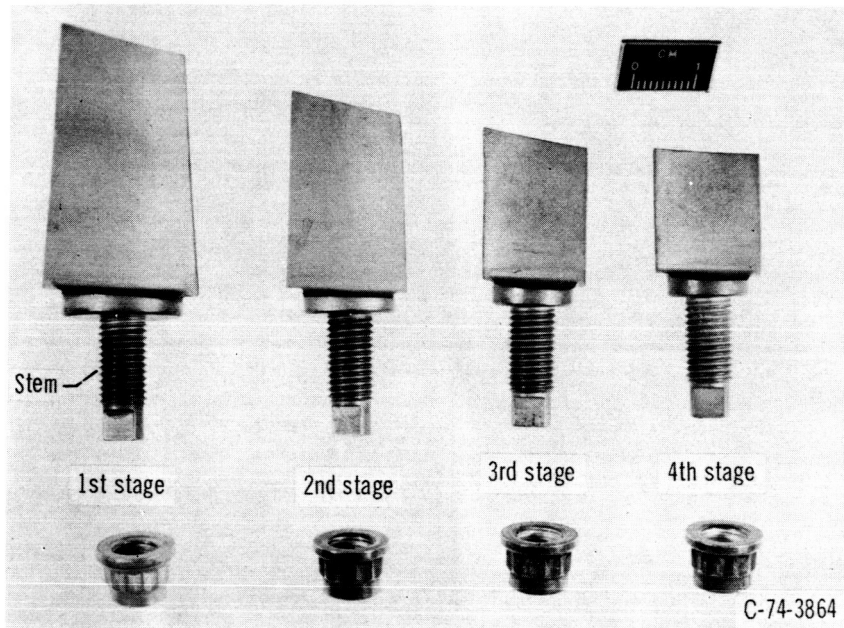
Figure 6. - Vane from each of four compressor stator stages.

Without vanes installed

Stator vanes

With vanes installed
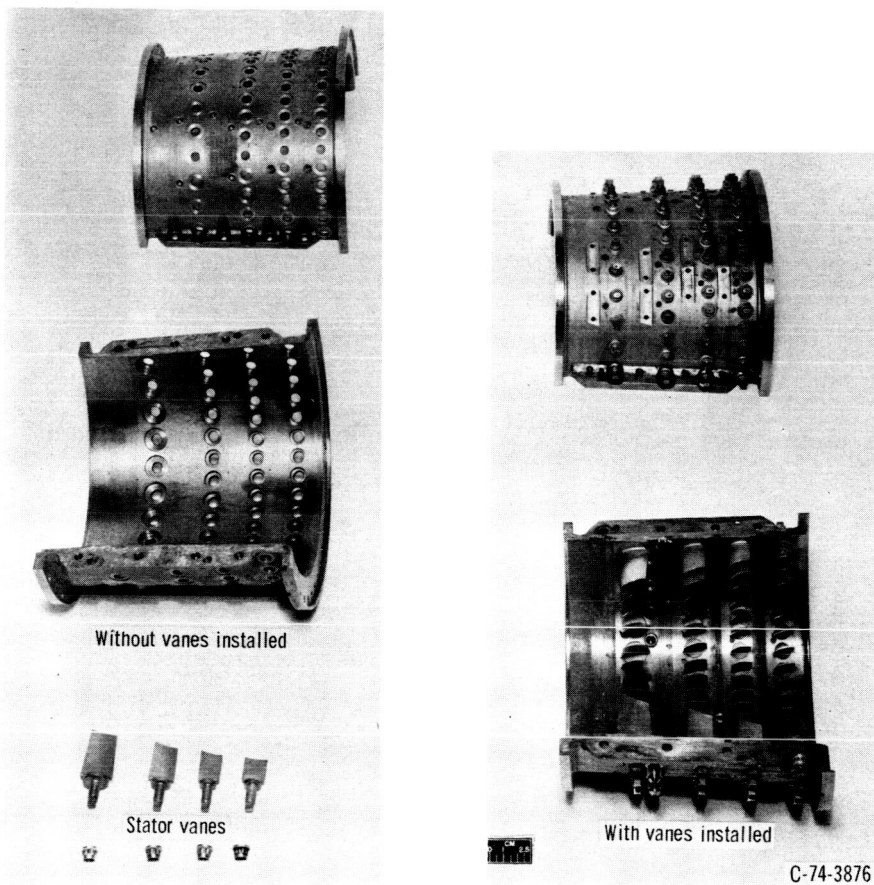
Figure 7. - Compressor casing halves with and without stator vanes installed.

Combustor housing

Combustor

Igniter

C-74-3872
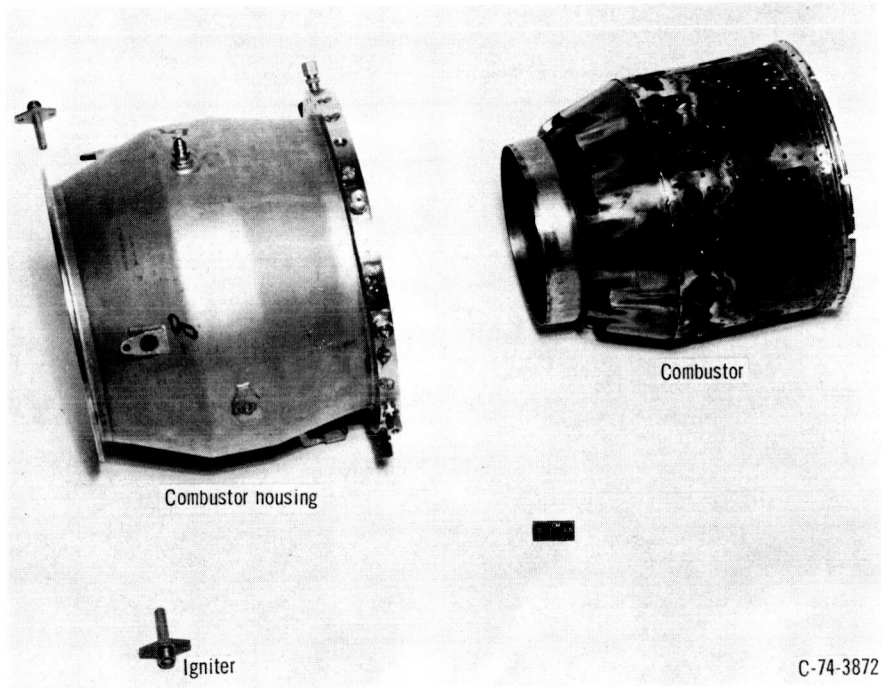
Figure 8. - Combustion section components.

Ring
support

Snout
(diffuser)

Fuel manifold

Fuel nozzles

Firewall

Inner liner

Outer liner

C-74-3868

(a) Components.

Outer liner

Snout

Ring support

C-73-433

(b) Downstream view.

Outer liner

Fuel-nozzle holder
and swirler assembly

Inner liner

C-73-432
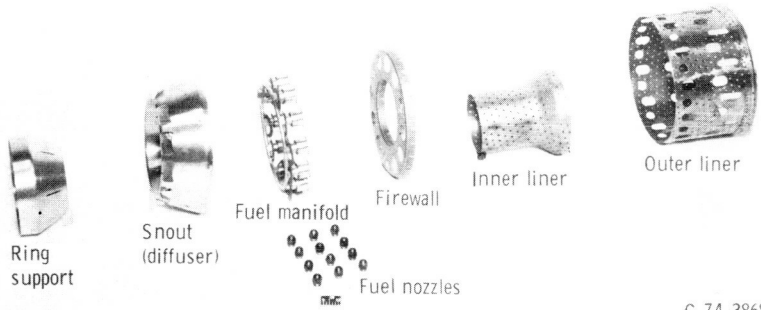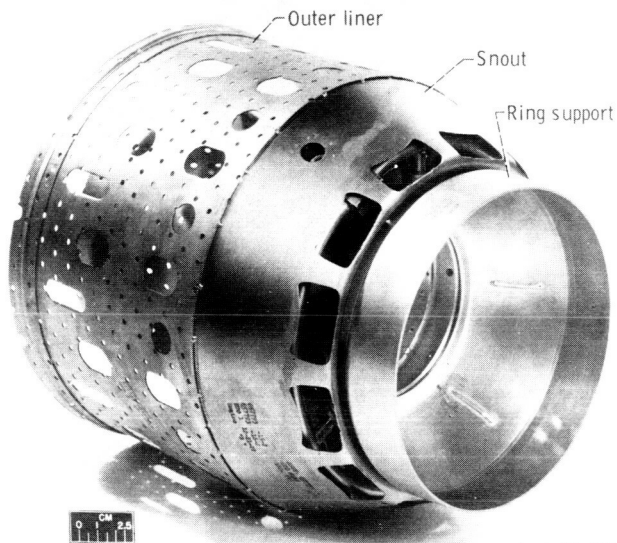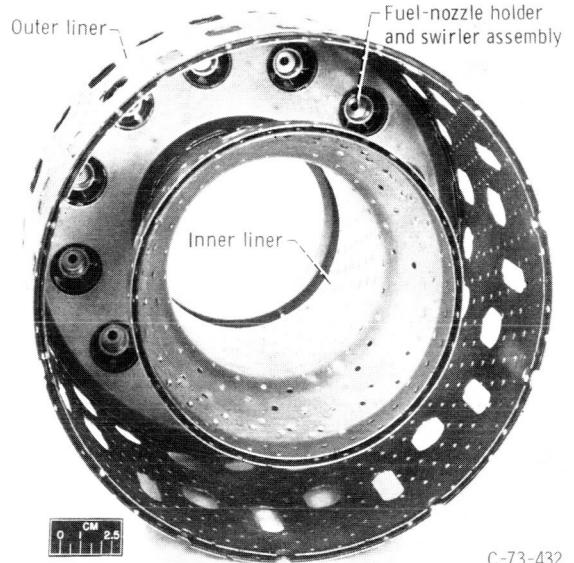
(c) Upstream view (fuel nozzles not installed).

Figure 9. – Combustor assembly.

As cast

Outer shroud
ring extension

Opening for
air impingement
start

Machined

As cast

Bolt hole

Stub shaft
(bearing surface)
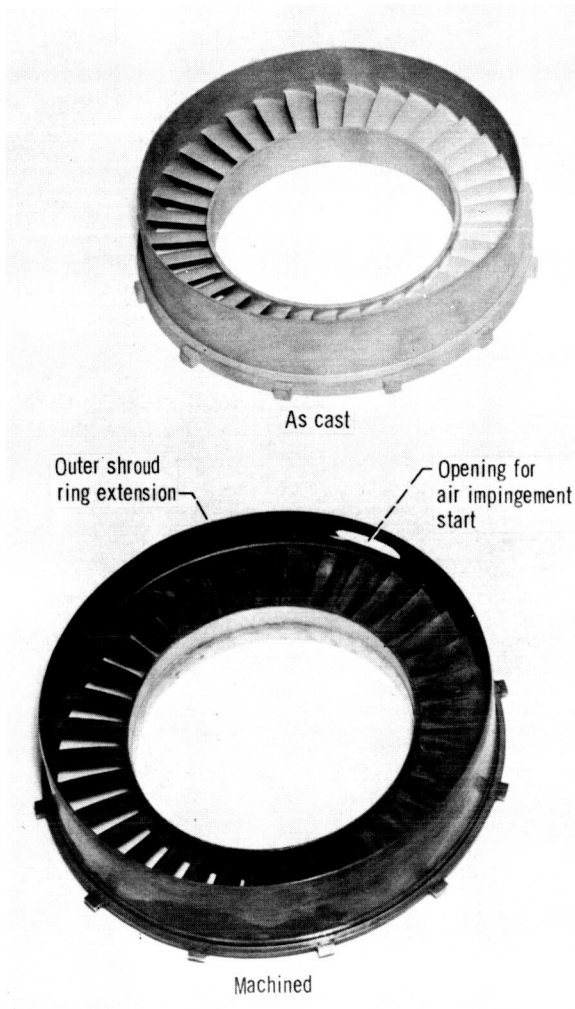
Machined

C-74-3869

C-74-3869

(a) Stator assembly.
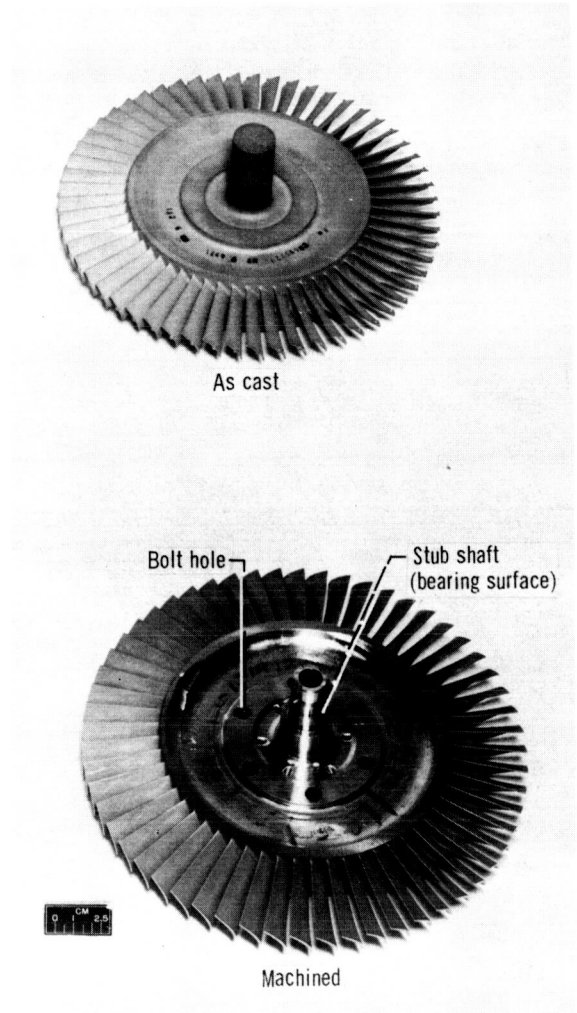
(b) Rotor assembly.

Figure 10. - Turbine components in as-cast and machined conditions.
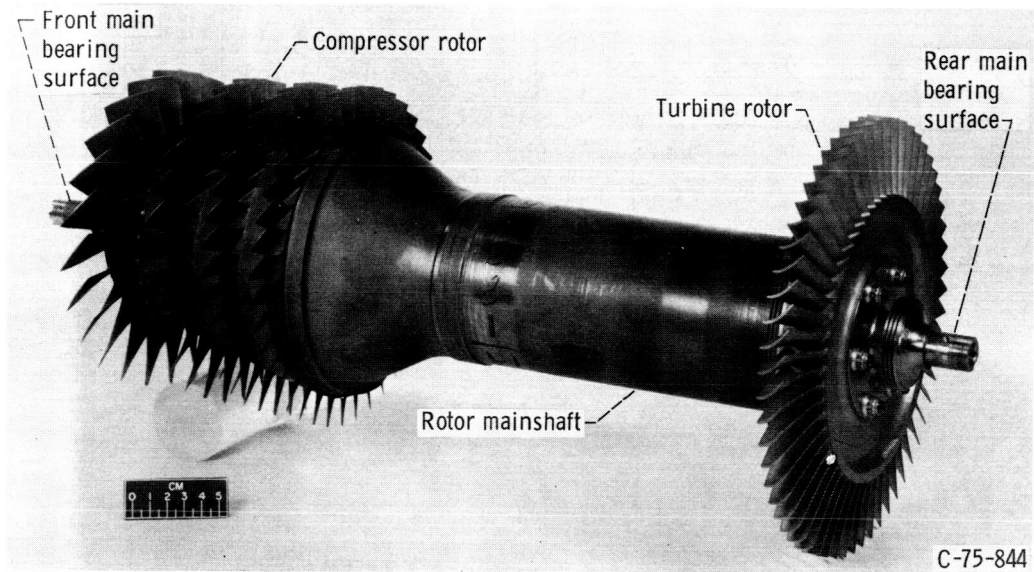
Figure 11. - Compressor-turbine rotor mainshaft assembly.

Oil mist

Exhaust duct

Combustor outer liner

Turbine stator

Turbine rotor

Combustor inner liner

Bearing housing

Rear main bearing

Combustor housing

CD-11981-07

(a) Schematic.

As cast

Exhaust duct

Bearing housing
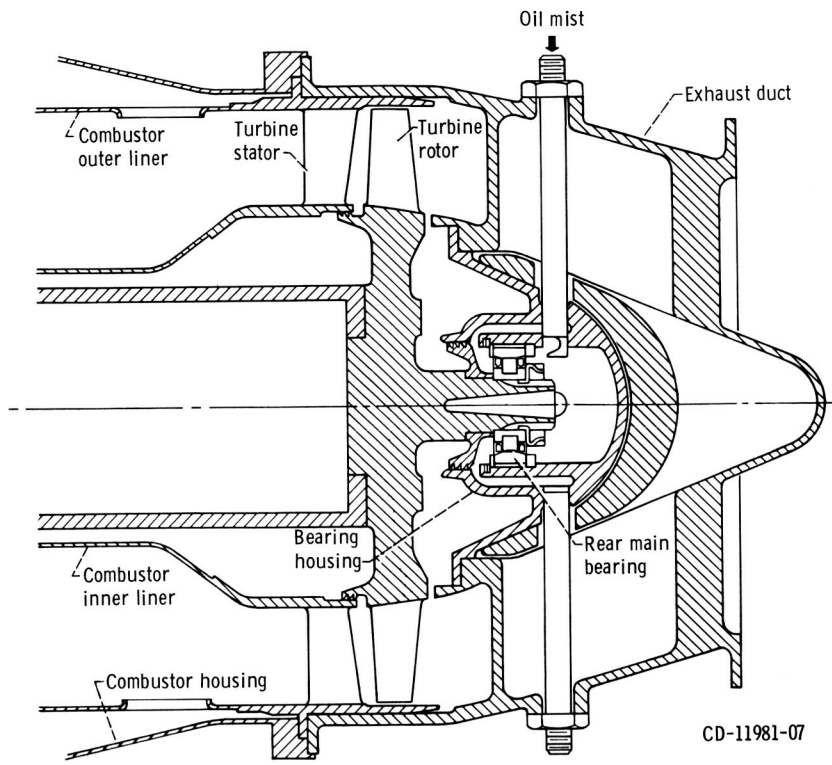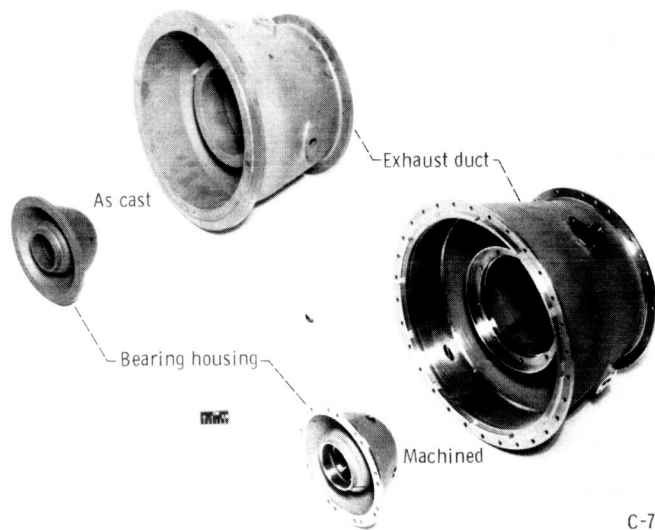
Machined

C-74-3879

(b) Exhaust duct and rear bearing housing in as-cast and machined conditions.

Bearing parts

Split ring adaptor

Turbine stator

Turbine rotor

Air deflector

Air seal

Bearing housing

Exhaust duct

Exhaust nozzle
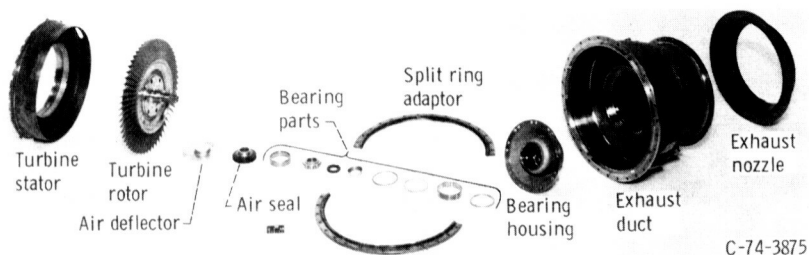
C-74-3875

(c) Associated hardware.

Figure 12. – Turbine and exhaust sections.

(a) Front main bearing.

(b) Rear main bearing.
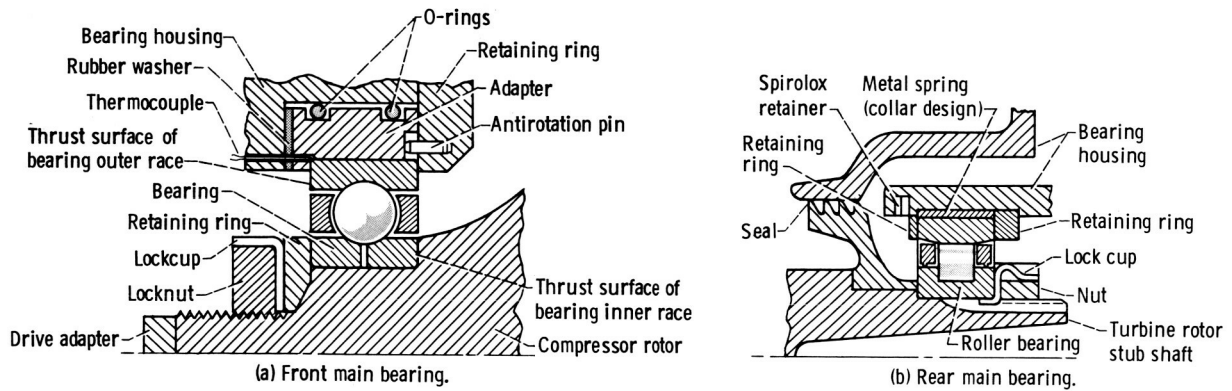
Figure 13. – Bearing-mount designs.

CD-11989-07
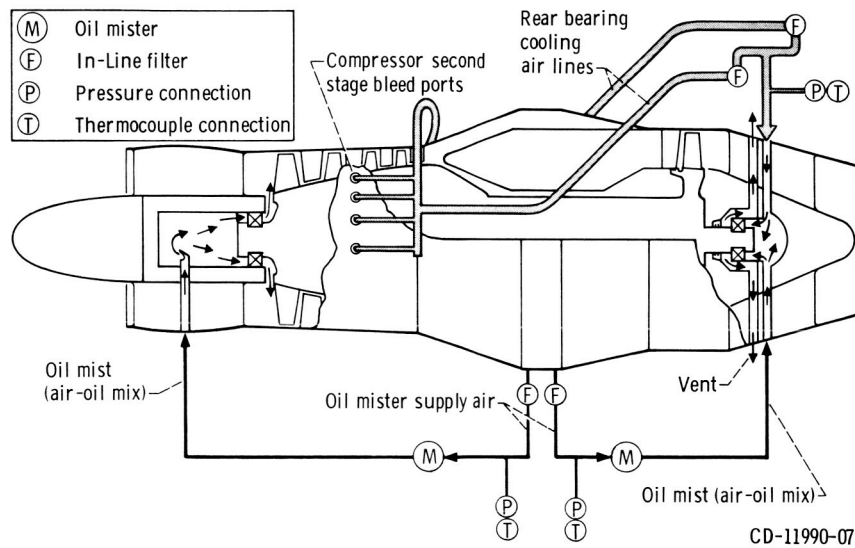
(a) Schematic.

CD-11990-07

C-74-3878

(b) Oil mist generators and associated cooling and lubrication lines.

Figure 14. – Engine bearing cooling and lubrication system.
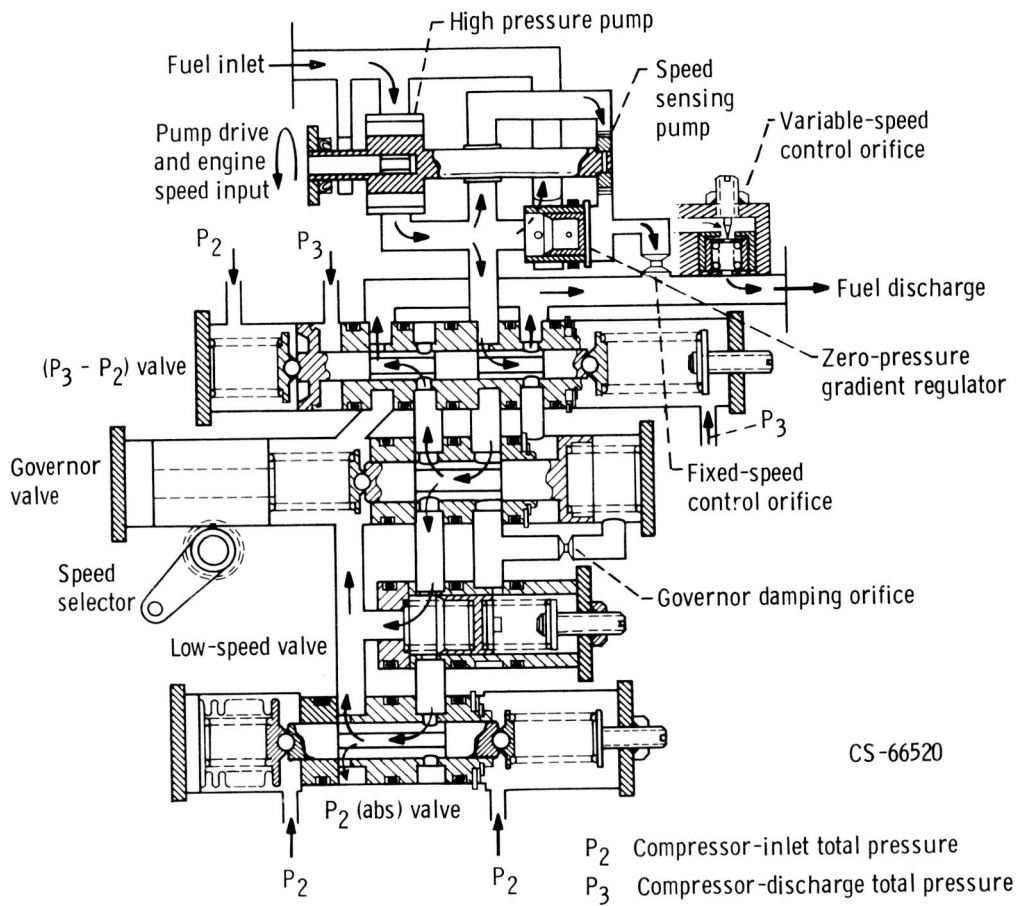
Figure 15. - Schematic of simplified fuel control.

High pressure pump

Fuel inlet

Speed sensing pump

Variable-speed control orifice

Pump drive and engine speed input

P_2

P_3

Fuel discharge

$(P_3 - P_2)$ valve

Zero-pressure gradient regulator

P_3

Governor valve

Fixed-speed control orifice

Speed selector

Governor damping orifice

Low-speed valve

CS-66520

P_2 (abs) valve

P_2

P_2

P_2 Compressor-inlet total pressure

P_3 Compressor-discharge total pressure

(a) Alignment of mainshaft with inlet section.
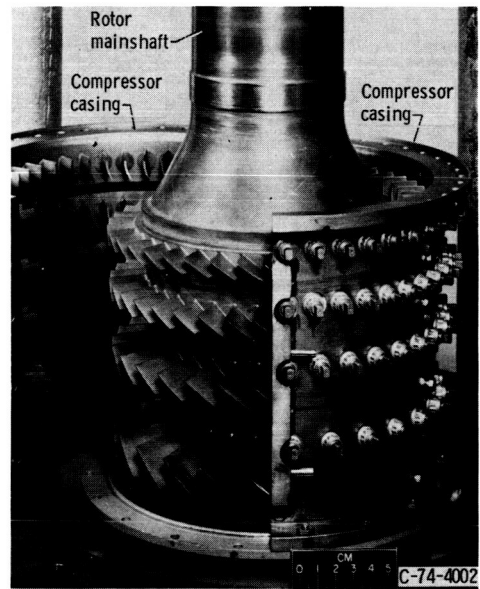
(b) Installation of compressor casing halves.

Figure 16. – Various stages of engine assembly.
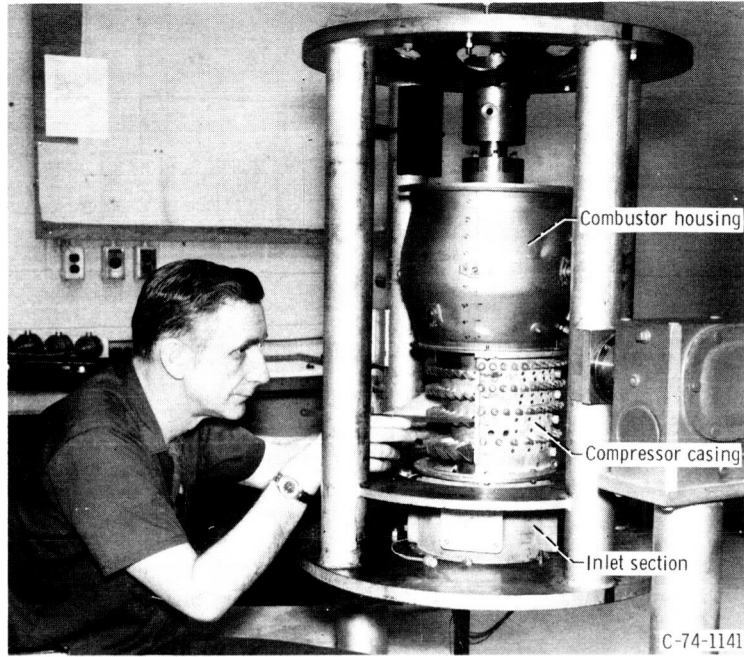
(c) Installation of combustor section.
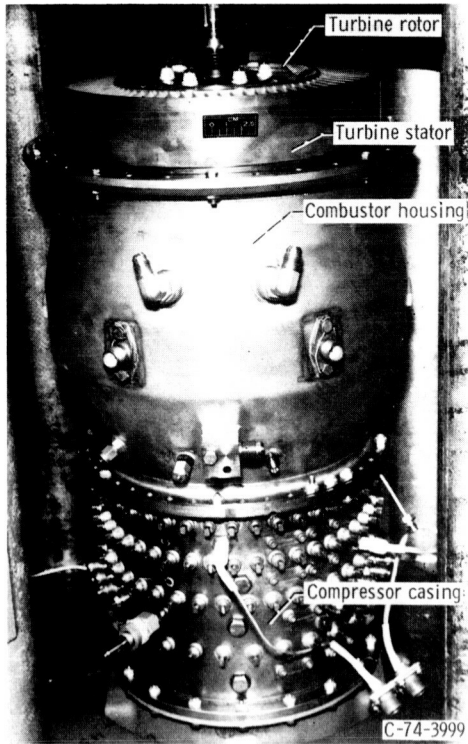
(d) Installation of turbine section.
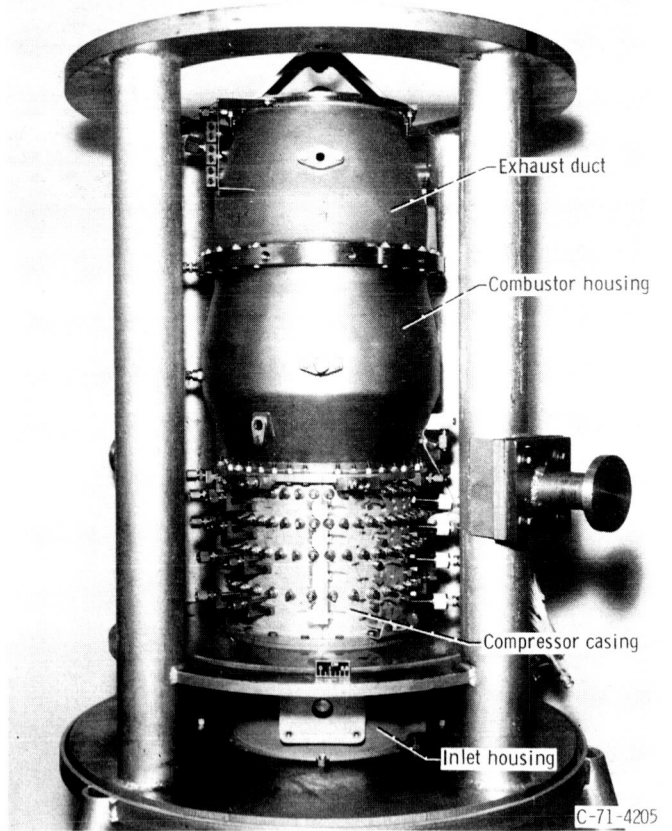
(e) Installation of exhaust section.

Figure 16. – Concluded.
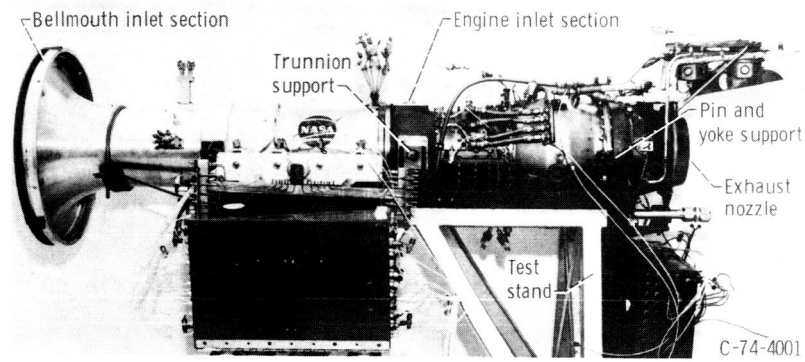
(a) Before installation in test cell.
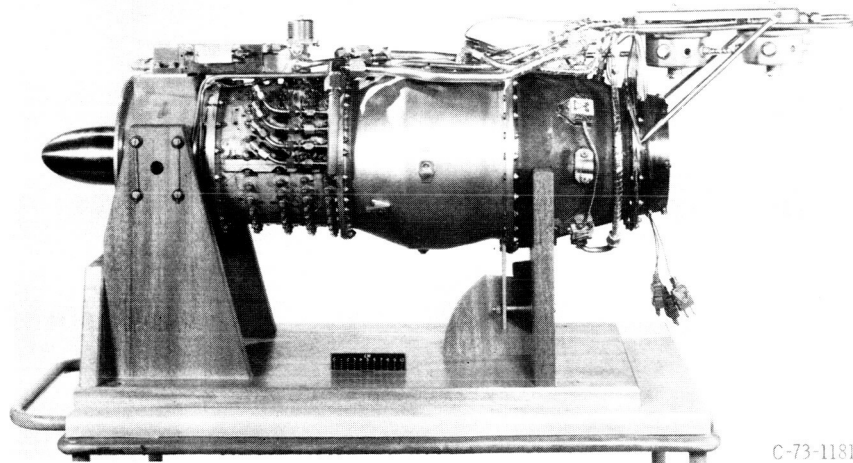
(b) Basic engine ready for shipment.

Figure 17. – Assembled engine.
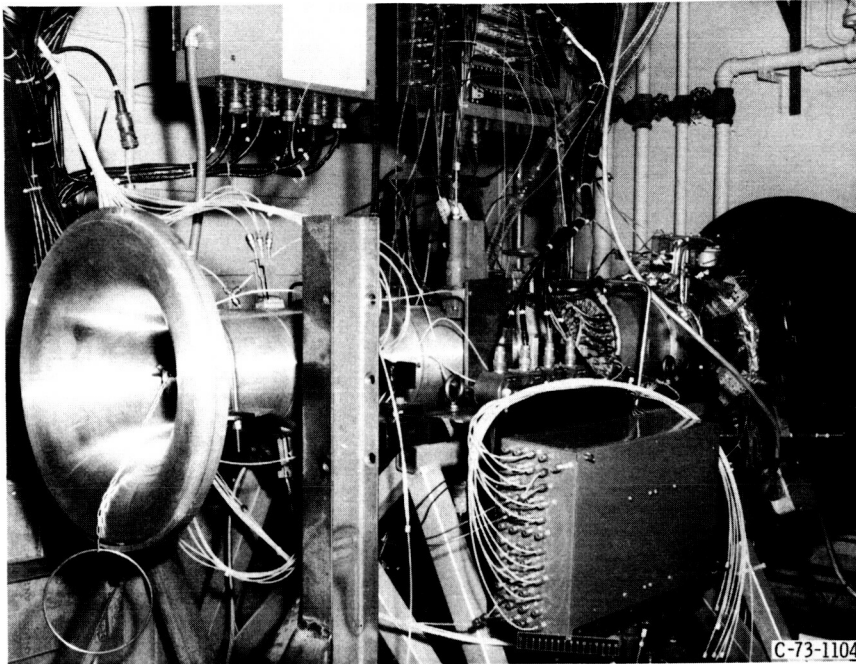
Figure 18. - Engine installed in facility for sea-level-static testing.
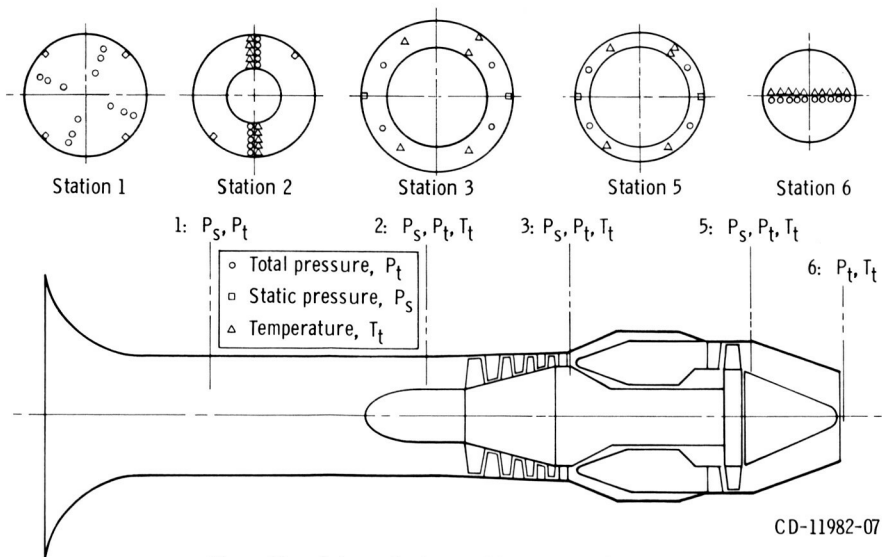
Figure 19. - Primary instrumentation station locations.

(a) Temperature at station 5.

(b) Temperature at station 6.

(c) Engine speed. Rated speed, 35 170 rpm.

Time, sec

(d) Fuel flow.
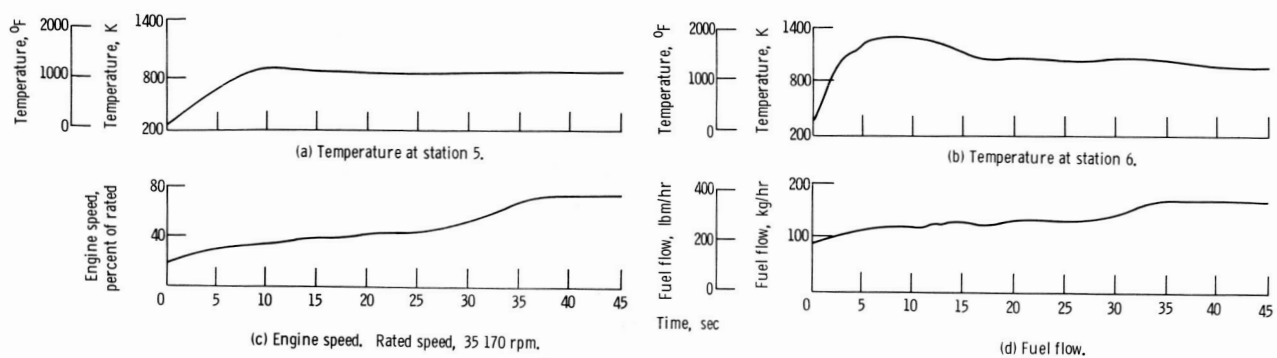
Figure 20. - Engine starting characteristics.
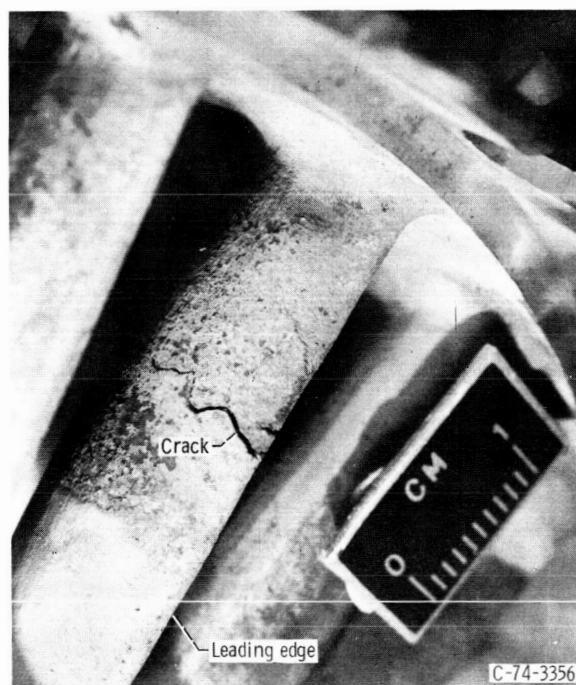
Figure 21. - Crack in leading edge of turbine stator vane.
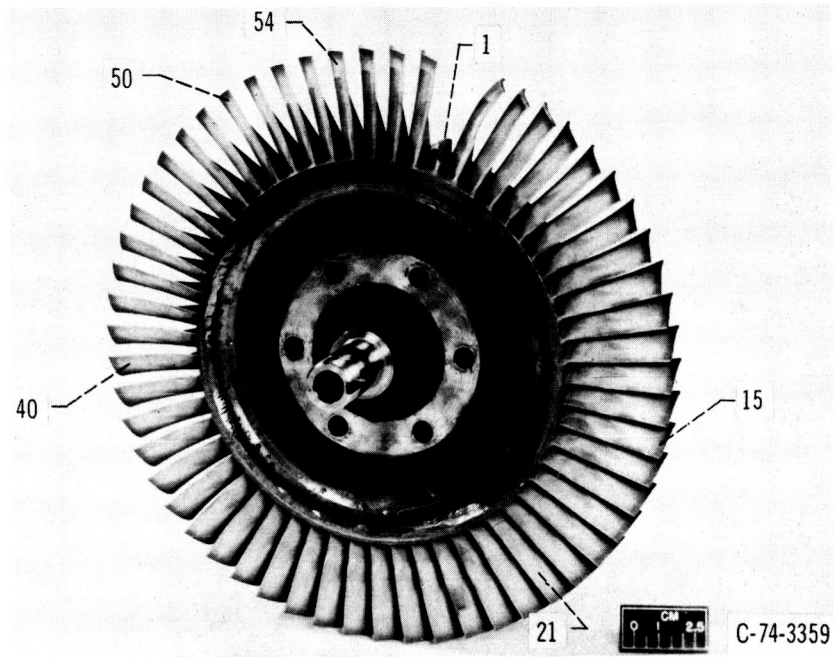
(a) Overall view.
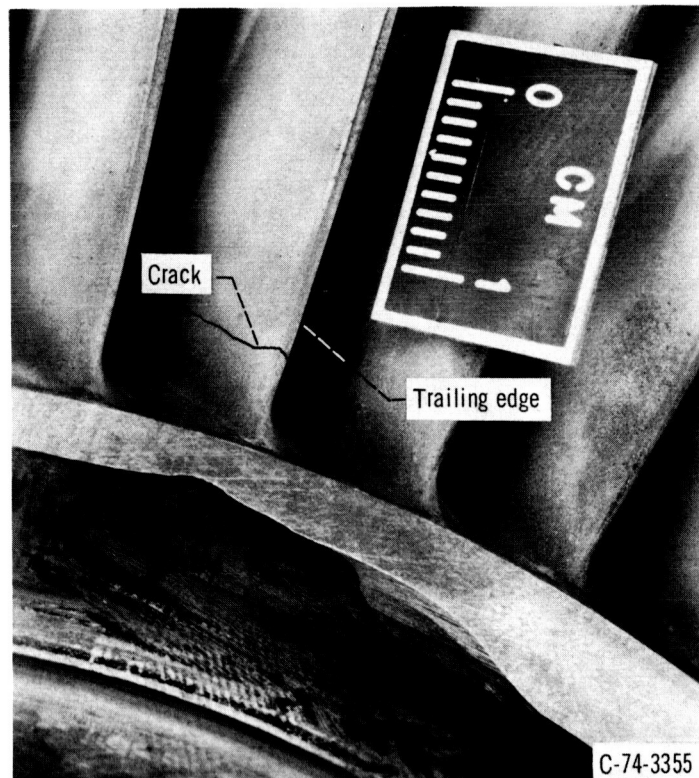
(b) Closeup of crack in trailing edge of blade 21.

Figure 22. - Turbine blade failures.
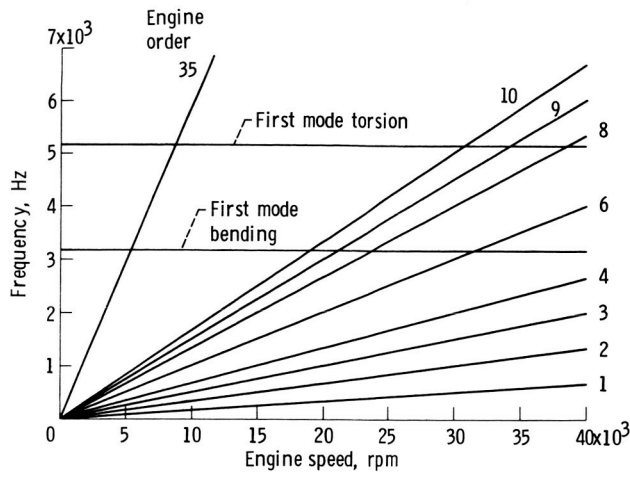
Figure 23. - Turbine rotor blade interference diagram.
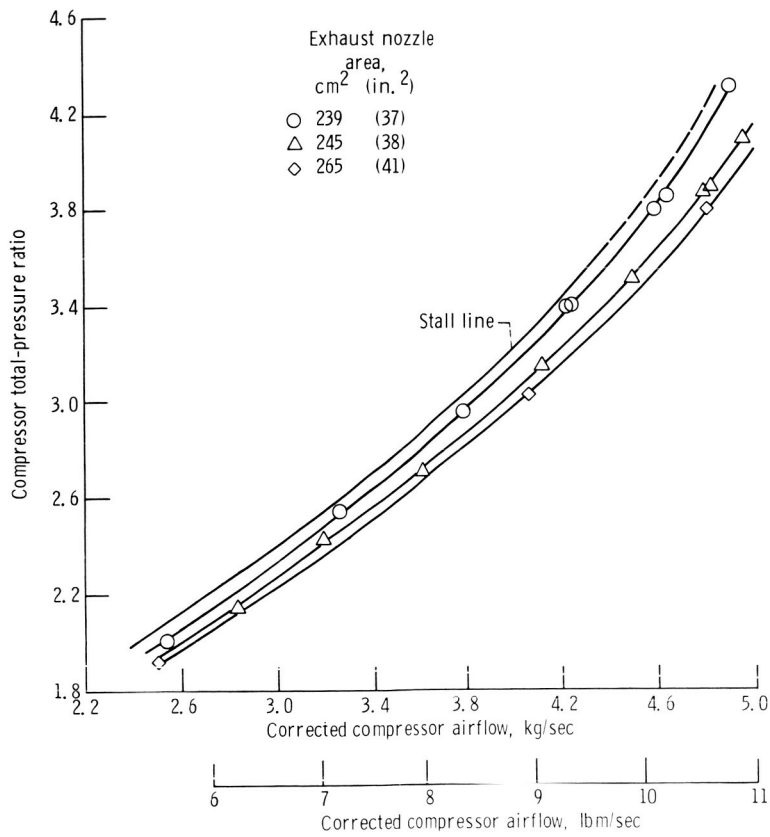
Figure 24. - Engine operating lines for three exhaust nozzle sizes.
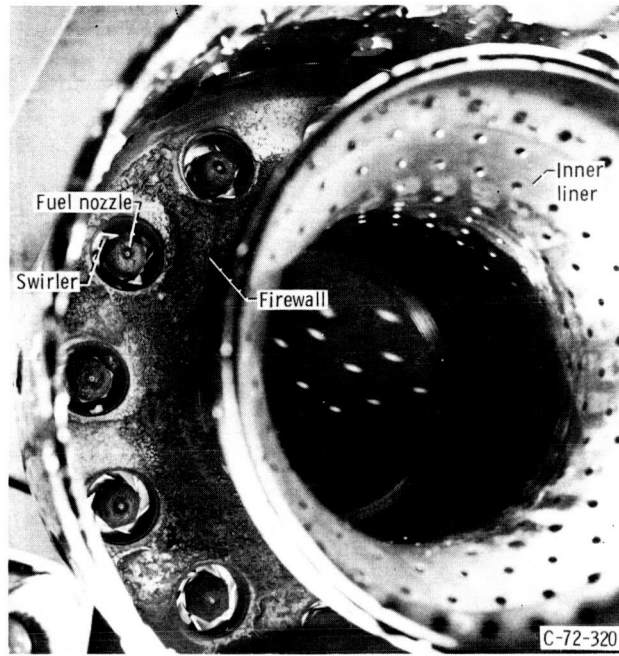
(a) Overall view.
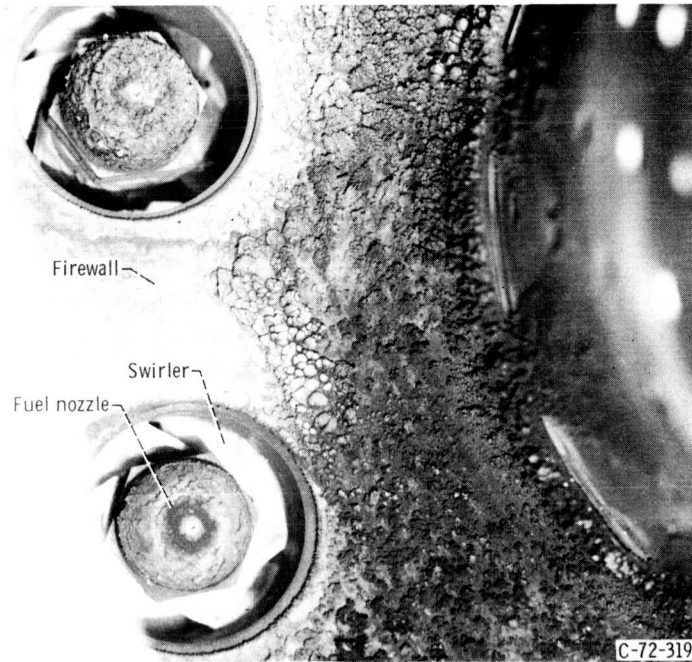
(b) Closeup.

Figure 25. - Carbon buildup in combustor assembly.

(a) First mode (cylindrical).

(b) Second mode (conical).
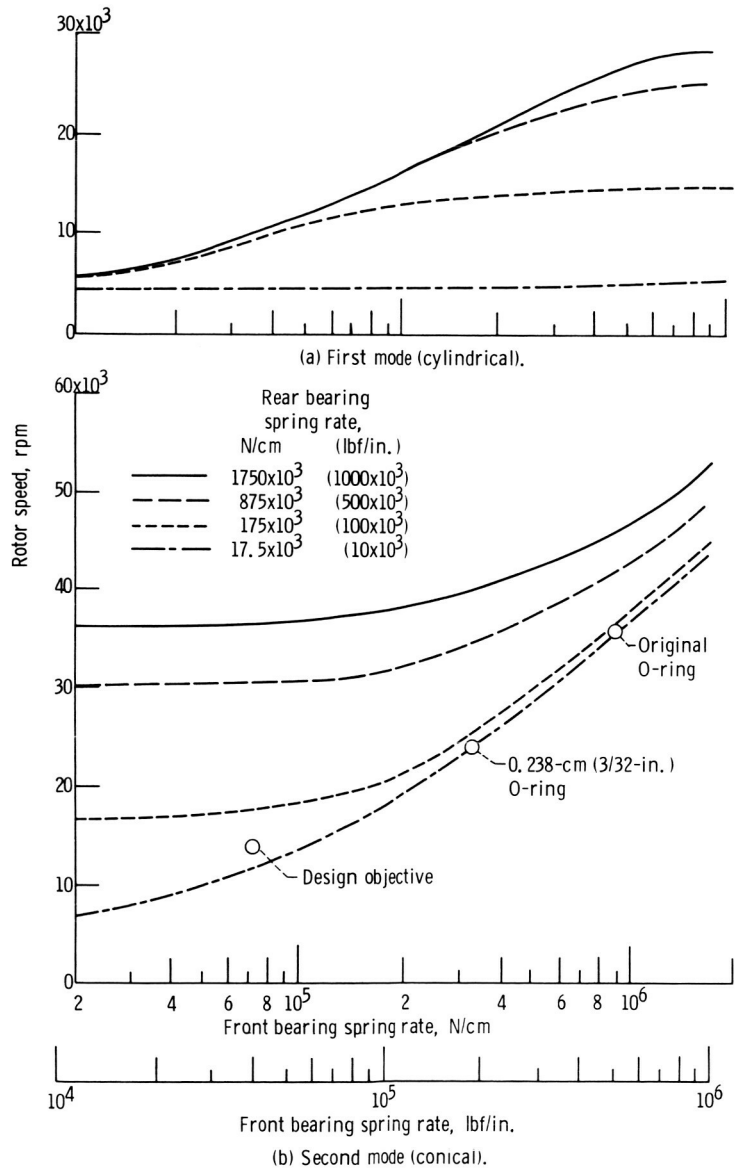
Figure 26. - Engine rotor critical speeds.
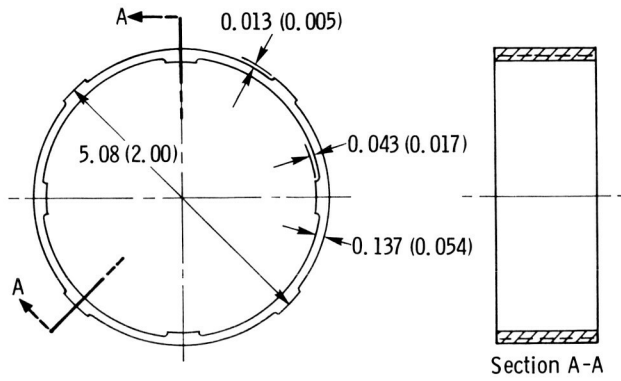
Figure 27. - Metal spring design (collar) for rear bearing mounting system. Material, AMS 6322. (All dimensions are in cm (in.).)
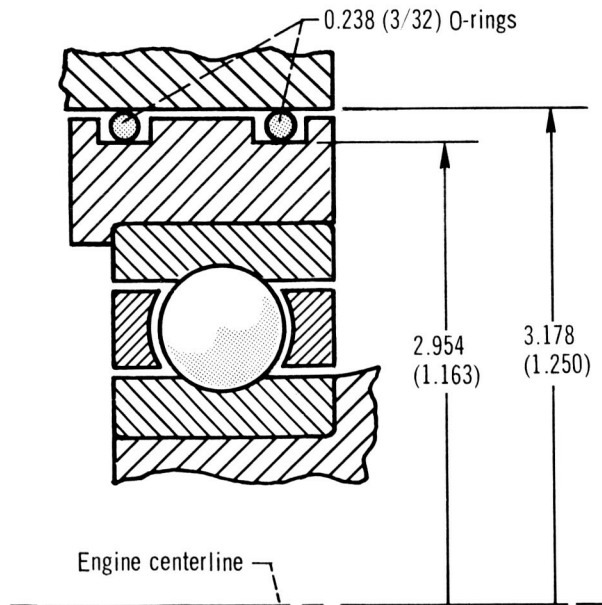
Figure 28. - Radial compression of O-rings of front bearing mounting system. (All dimensions are in cm (in.).)

(a) Front bearing horizontal vibration; 0 to 1000-hertz pass filter.

(b) Front bearing vertical vibration; 0 to 1000-hertz pass filter.

(c) Rear bearing vertical vibration; 0 to 1000-hertz pass filter.

(d) Rear bearing horizontal vibration; 0 to 1000 hertz pass filter.
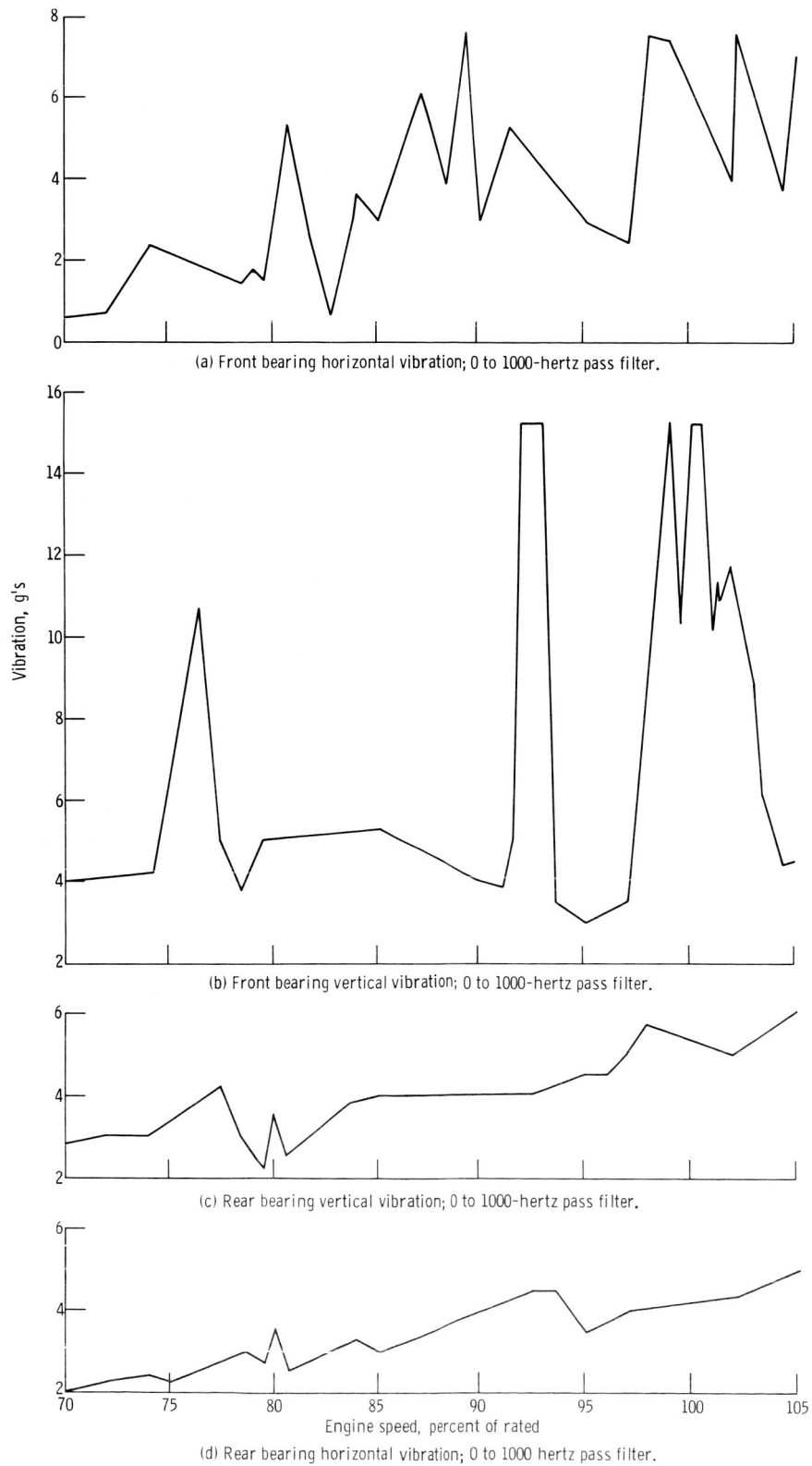
Figure 29. - Typical engine vibration levels at sea-level - static conditions.

Engine speed, percent of rated

Vibration, g's
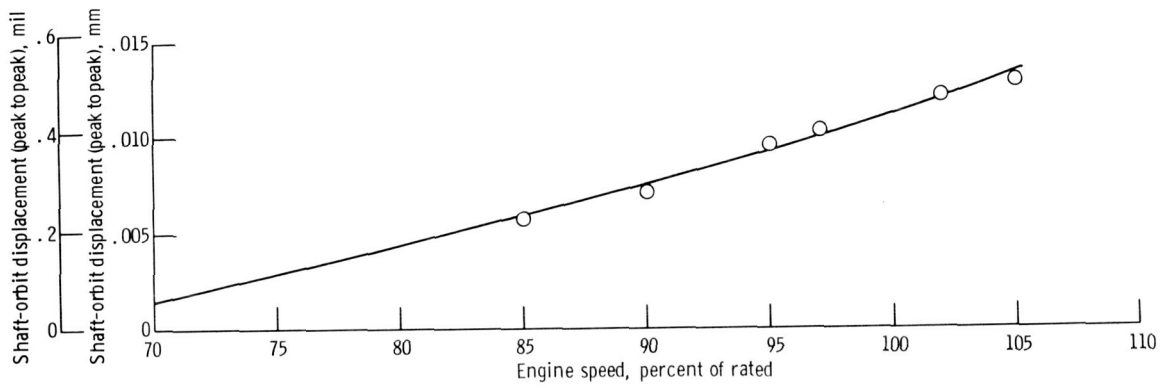
Figure 30. – Typical shaft displacement for engine operating range at sea level-static conditions.